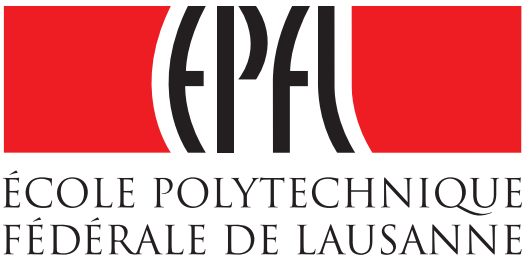

Experimental Investigation of Fast Ion Dynamics in Torpex Toroidal Plasma

Master project, Physics section
Spring semester 2010

Author: Boris Roulet

Supervisors:
Prof. A. Fasoli
and
Dr. Ivo Furno

CRPP-EPFL
Lausanne
July 15, 2010

Contents

1 Introduction **5**
- 1.1 Particles Drift . . . 6

2 Experimental Setup **9**
- 2.1 TORPEX . . . 10
  - 2.1.1 Plasma Confinement . . . 11
  - 2.1.2 Plasma Production . . . 11
- 2.2 HEXTIP . . . 12
  - 2.2.1 Typical Investigated Plasma . . . 12
  - 2.2.2 Interchange Instability . . . 14

3 Fast Ions Source **15**
- 3.1 Fast Ions Emitter . . . 15
  - 3.1.1 Test of the Emitter . . . 16
  - 3.1.2 Test of the Fast Ions Emitters . . . 17
- 3.2 Fast Ion Source . . . 20

4 Double Gridded Energy Analyzer **25**
- 4.1 Synchronous Detection . . . 25
- 4.2 Previous Setup . . . 28
- 4.3 New Setup . . . 28
  - 4.3.1 Look-in Device . . . 31
- 4.4 Moving System . . . 36

5 Experimental Results **39**
- 5.1 Experiments Without Plasma and Without Magnetic Field . . . 41
  - 5.1.1 Profile With 300 eV . . . 44
  - 5.1.2 Profile With 500 eV . . . 46

5.1.3 Profiles Measured with the 3^{rd} Emitter 47
5.2 Experiments Without Plasma and With the Magnetic Field . 48
5.3 Experiments With Plasma 50
5.3.1 Profile With 300 eV 50
5.3.2 Profile With 500 eV 52
5.4 Post deadline measures 55

6 Discussion **57**
6.1 Comparison With Simulation 57
6.1.1 Description of the Code 57
6.1.2 Calibrations Simulation 59
6.2 Capacitive Effect 61
6.2.1 Effect of the peaks 64

7 Conclusion and Outlook **69**

A Tests of the Emitters **73**

B Plan of the Source's Toroidal Moving System **79**

C Mode d'emploi montage de la source **81**
C.1 Piece à disposition 81
C.2 Préparation des grilles 82
C.3 Préparation de l'émetteur 84
C.4 Assemblage de la source 85
C.5 Assemblage au système de support 88
C.6 Conclusion 89

D Câblage **91**
D.1 Boitier du détecteur 91
D.2 Lock-in 92
D.3 Source 93

Chapter 1

Introduction

The fusion in the future fusion reactor is lead by the reaction:

$$D + T \rightarrow He(3.52MeV) + n(14.1MeV) \tag{1.1}$$

This type of fusion is the most probable fusion due to the large cross section at a temperature of 100 keV. We need to heat the plasma to reach this temperature.

The plasma can first be heated by ohmic heating. The plasma resistivity is proportional to $T^{-\frac{3}{2}}$. When the plasma temperature is too high, the plasma resistivity goes down to zero. The plasma can then be heated by injection of microwave. When the number of fusions per second is high enough the plasma will be self-heated by the alpha particles (produced in the reaction 1.1) with energies well above the background plasma, this state is called ignition. It is then very important to understand how the particles will influence the plasma and how the low-frequency plasma turbulence will influence the dynamics of the particles.

It's very hard to investigate this kind of dynamics in a tokamak, the plasma temperature is too high. Experimental investigations have already been made on the LAPD in the university of California [2][3][4] and at the EPFL Lausanne [1]. The goal of this diploma is to investigate these dynamics in the TORPEX (TORoidal Plasma EXperiment) dedicated to basic plasma experiments where the plasma temperature is about 5 eV allowing investigation with small devices.

We will use a Li-6+ source which consists of a aluminosilicate Li-6+, housed in a boron nitride cylindrical casing to generate fast ions on the TORPEX. This source can produce particles with energy between 100 eV and 1 keV. It will be used with a probe. The probe has a 2D resolution.

This diploma is the followup to the thesis, "Interaction of Supra-Thermal Ions with Turbulence in a Magnetized Toroidal Plasma" [1] lead by Gennady Plyushchev until 2009. Our first idea was to use the same material and reproduce the experiments changing the energy of ions in the source and moving the source at different points of TORPEX to obtain a 3D resolution. Problems arose when we first tried to use the emitter in the source. We then realized that some problems with the global experimental setup make it hard to take measures. We then decided to change the setup to optimize the quality of the results and the time to make a global fast ion profile.

This new setup allows us to make a profile in a relatively short time, 10 minutes to 1 hour where we previously needed half a day. We will present here the new setup and the first results we obtained with this setup.

In this diploma, we will first present, in chapter 2, the TORPEX experiment. In the third chapter, we describe how we emit fast ions by presenting the fast ion emitter, the source and the test made to check the quality of the material. In chapter four, the detector is described. First the previous setup, then all the changes we have made on the probe. In the next chapters, we present and discuss the profiles made with the fast ion source and the probe. The next chapter presents a design for a moving system for the source in the toroidal direction.

1.1 Particles Drift

As said before, the most important topic of this diploma is how charged particles with high energy influence and be influenced by the plasma. To confine the plasma we use magnetic field (see chapter 2). The trajectories of charged particles are influenced by the magnetic field. We present here a small review of the drift of charged particles in a magnetic field.

Let's consider a plasma confined within a magnetic field without an elec-

tric field and subjected to a constant force F. We can then rewrite the equation of motion as:

$$m\frac{dv}{dt} = F + q(v \times B) \tag{1.2}$$

We can separate this equation in two, one parallel to B (written $\|$) and one perpendicular to B (written $\perp$):

$$\frac{dv_\|}{dt} = \frac{F_\|}{m} \tag{1.3}$$

$$\frac{dv_\perp}{dt} = \frac{F_\perp}{m} + \frac{q}{m}(v_\perp \times B) \tag{1.4}$$

To solve the equation 1.4, we introduce the drift velocity v_d given by:

$$v_d = \frac{1}{q}\frac{F_\perp \times B}{B^2} \tag{1.5}$$

As v_d is constant ($F\perp$ and B are constant), we can replace $v_\perp$ by $v_\perp = v'_\perp + v_d$ in equation 1.4 an so:

$$\frac{dv'_\perp}{dt} = \frac{q}{m}(v'_\perp \times B) \tag{1.6}$$

The particles have a cyclotron movement in a referential that moves with the velocity v_d. The radius of this cyclotron movement, R, called the Larmor radius is:

$$R = \frac{mv_\perp}{|q|B} \tag{1.7}$$

Where m is the mass of the charged particle, $v_\perp$ is the velocity component perpendicular to the magnetic field B and q the charge of the particle.

Let's consider a magnetic field with a radius. A particle in this magnetic field will have two drifts. One in the moving referential, $v_{D1} = \frac{1}{q}\frac{F_c \times B}{B^2}$ (see equ. 1.5) and one due to the radial variation of B. If B decreases radially in 1/R, the perpendicular drift becomes:

$$v_{D2} = \frac{mv_\perp^2}{2B^2q}\frac{R \times B}{R^2} \tag{1.8}$$

The total drift becomes:

$$V_D = v_{D1} + v_{D2} = \frac{m}{q}\frac{1}{R^2B^2}(R \times B)\left[v_{\parallel}^2 + \frac{1}{2}v_{\perp}^2\right] \tag{1.9}$$

This result means that it's possible to confine plasma with a toroidal magnetic field like it's done on TORPEX (see chapter 2).

Chapter 2

Experimental Setup

All experiments in plasma conditions will be done, for this diploma, in the TORPEX device. In this chapter, we make a global description of this experiment, which started operated in 2003 at the CRPP-EPFL, Lausanne.

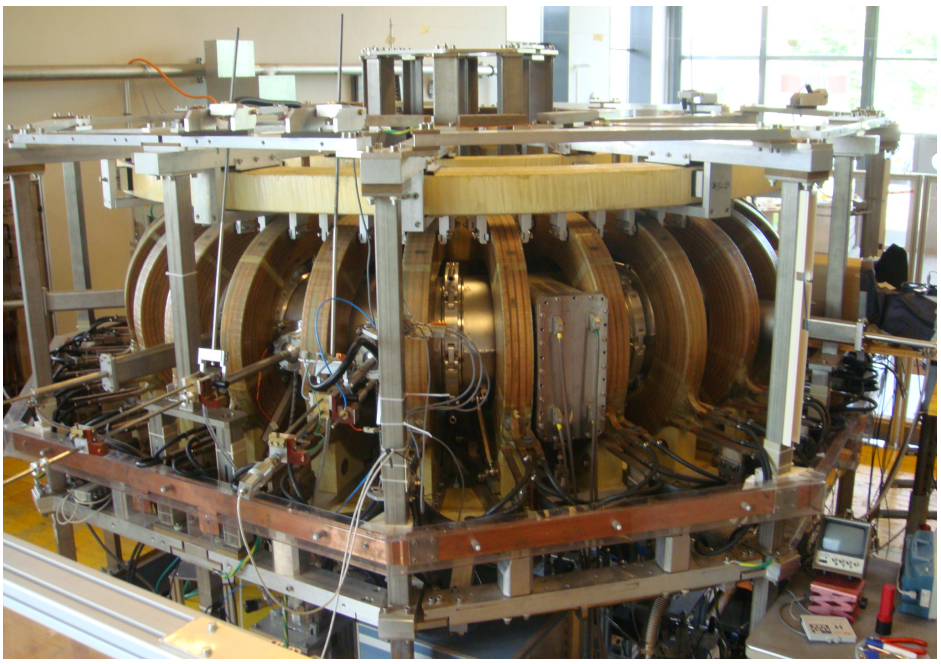

Figure 2.1: The TORPEX device.

2.1 TORPEX

The TORPEX is a basic plasma physics experiment. Its primary goal is the investigation of turbulence, plasma instability and transport in a simplified environment. The machine can be divided into four parts; the vacuum chamber, the magnetic coils, the magnetron and the diagnostics. The temperature and the plasma density is lower in the TORPEX than in a tokamak. This allows easier access for the diagnostic and a global investigation of the plasma produced in the device. We are not confined to the border of the plasma, but are able to put probes in the center of the plasma.

The vacuum chamber of TORPEX is a torus with a major radius of 1 m and a minor radius of 0.2 m. The torus is divided into 12 sectors, 4 of them are movable and can be removed from the machine to install diagnostics directly inside the torus. On the other sector, diagnostics can be installed on different points, about 3 every 22.4 cm (12.86^o). They can be installed on the low field side (LFS), the upper side of the machine or under it. To investigate the fast ion dynamics, we will only use flasks on the LFS. On the following picture, we can see the source and the probe installed on TORPEX. The distance between them is about 22.4 cm.

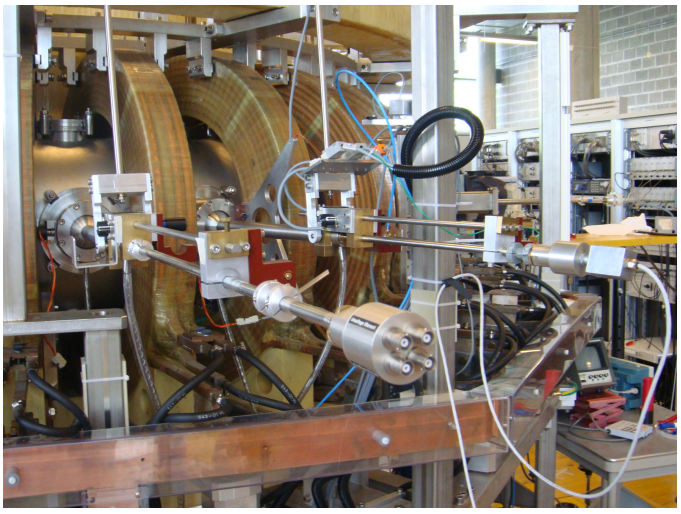

Figure 2.2: The source (foreground) and the probe (on the left) installed on TORPEX.

The vacuum in the chamber is maintained by 4 turbomelcular pumps, backed by 4 primary pumps. The vacuum in the vessel is about $3 \cdot 10^{-7}$ mbar. During experiments, gases are injected into the vacuum chamber; in the TORPEX it's commonly Hydrogen, Argon, Neon, Nitrogen, Helium and Deuterium. The gas injection rate can be adjusted. For the experiments we have adjusted the injection to have a pressure of about 10^{-4} mbar.

2.1.1 Plasma Confinement

As said before, the plasma is confined in TORPEX with magnetics coils. There are 28 toroidal magnetics coils that can produce a magnetic field up to 0.1 T on the axis. This magnetic field decrease when the radius increase. As said in chapter 1, particles have a drift velocity $V_D = v_{D1} + v_{D2} = \frac{m}{q}\frac{1}{R^2B^2}(R \times B)\left[v_\parallel^2 + \frac{1}{2}v_\perp^2\right]$. This drift depends on the sign if the charges, this mean that ions and electrons drift in the opposite direction. This creates an electric field E. And therefore particles suffer the effect of an other drift $v_{E\times B} = \frac{E\times B}{B^2}$. Adding a vertical magnetic field, B_z, creates a Lorentz force on the charges: $F = I_p \times B_z$. By choosing the orientation of B_z, we can choose the direction of this force to bring back particles to the center and upgrades the plasma confinement. On TORPEX, this magnetic field is created by horizontals coils who provide a vertical magnetic field up to 5 mT.

2.1.2 Plasma Production

The plasma is produced and sustained by injection of microwaves. We can use two different magnetrons to produce the microwaves that are injected in TORPEX. Both magnetrons used ordinary mode microwaves of 2.45 GHz which corresponds to the electron cyclotron resonance in a toroidal magnetic field of 87.5mT [1].

One of the magnetron launches microwaves from the LFS. Its maximum power is of 30kW in pulse mode. The duration of the pulse is up to 100ms. In continuous mode, the power is up to 5kW, but the minimum is 200W [1].

The other magnetron launches waves from the bottom of TORPEX with a maximum of power of 1.2kW. It can be used to produce weakly turbulent plasmas [1].

2.2 HEXTIP

To investigate the fast ion dynamics, we used a fast ion source (see chapter 3) and a gridded energy analyzer (see chapter 4). There are many other diagnostics installed on TORPEX. We used the HEXTIP (HEXagonal Turbulent Imaging Probe) to characterize the plasma used for the experiments. The HEXTIP is a two-dimensional Langmuir probe array, consisting of 86 tips. It's used to measure the density and floating potential profiles with a resolution of 3.5 cm.

2.2.1 Typical Investigated Plasma

We can see in the following figure the typical plasma used to investigate the fast ion dynamics.

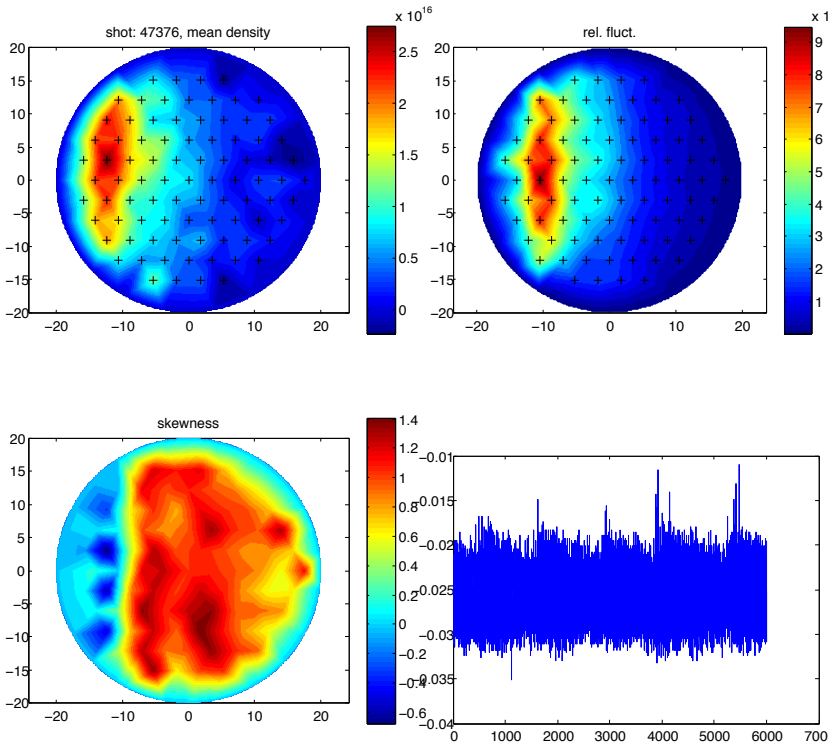

Figure 2.3: Mean plasma profile used during experiments.

The plasma source is localized on the high field side (HLF). The quantity of plasma produced for $r > 5cm$ is negligible. The next figure shows 2D profiles of the time-averaged electron pressure $\bar{p}_e = \bar{n}_e \bar{T}_e$, plasma potential $\bar{V}_{pl}$ and $E \times B$ velocity $\bar{v}_{E\times B}$ obtained from Langmuir probe measurements.The plasma potential is calculated from $\bar{V}_{pl} = \bar{V}_{fl} + \mu \bar{T}_e/e$, where $\bar{V}_{fl}$ is the floating potential, $\bar{T}_e$ the electron temperature and $\mu = 3.1 \pm 0.6$ is determined experimentally. The $E \times B$ velocity is calculated from $\bar{v}_{E\times B} = (-\nabla V_{pl} \times B)/B^2$[5]. We can see that the electron pressure and the plasma potential decrease when r increases.

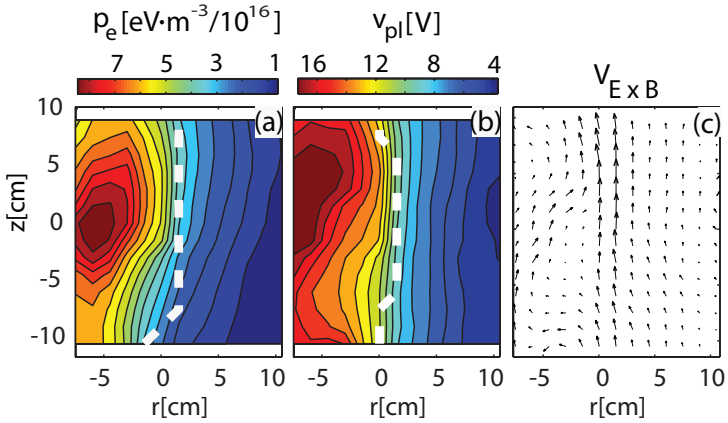

Figure 2.4: (a) Electron pressure,(b) plasma potential and (c) $E \times B$ velocity, picture taken in [5].

As we will see later, we can move the source to different positions, horizontally or vertically. For the experience we have chosen to put the source at the position (8,0). This means that the source will stand in a region where the plasma density is relatively small. This region, contained in $5cm \leq r \leq 15cm$ is called the blobs region. It's where the blobs, created by the interchange instability, will be propagated.

2.2.2 Interchange Instability

Interchanges instabilities appear at the limit of a plasma supported by a magnetic field B in a gravitational field, or in a gradient or curve of the magnetic field. Let's consider an independent force F. The direction of the force F is perpendicular to the limit of plasma and to B. This force introduces a drift of the particles, perpendicular to F and B (equ. 1.5), V_F. The ions and the electrons will derive in opposite direction and create a space charge in the border of the plasma. This space charge creates an electric field E, which creates a new drift V_E. This effect is illustrated in the next figure.

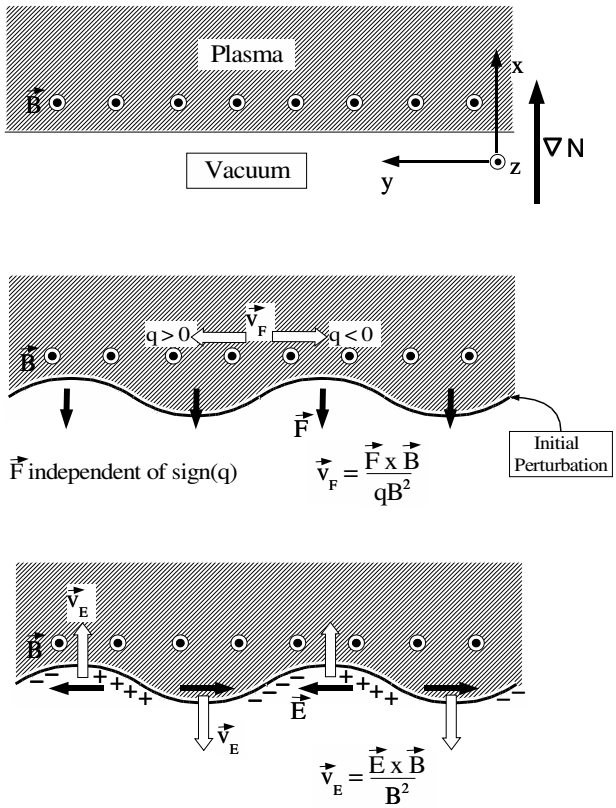

Figure 2.5: Illustration of the interchange instability, picture taken in [7].

This kind of instability leads to the creation of blobs. Blobs are ejected from the plasma.

Chapter 3

Fast Ions Source

The fast ions source is divided into two parts, the emitter and the source. The ions emitter will provide the ion beam, but isn't able to resist to the plasma conditions and won't provide a focus beam. The source is here to hold the emitter in the TORPEX and focus the beam with two aligned grids.

3.1 Fast Ions Emitter

The fast ions emitter we have used are provided by "Heat wave lab", from Watsonville, California, USA. These are aluminosilicate lithium ion emitter which provide beams of Li_6. The mains advantages are a very small size and are relatively easy to use.

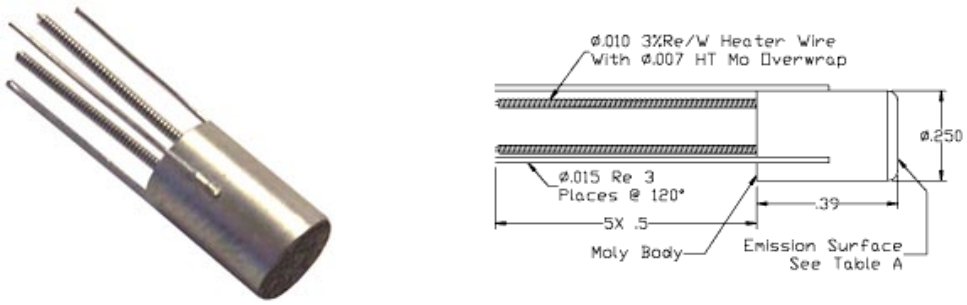

Figure 3.1: Fast ions emitter, Ø 0.25"

The emitters work at high temperature, about 1100^{o}C, with the principle of thermionic emission[1]. We then need to heat it. It's made with an internal

heating filament through which we pass a current. When the temperature is high enough, some ions are ejected from the surface of the emitter. To have a good emission, we need to set the emitter at a positive potential. The ions' current rise with the potential due to the Schottky effect [1].

The emitter consists of a heating filament, integrated in a small box. There is no connection between the filament and the box. The aluminosilicate lithium has been set on one side of the box. Three rhenium support struts are brazed on the box [6].

3.1.1 Test of the Emitter

Before mounting any emitter on the source, we need to test it alone in a small vacuum vessel. This small vessel, compared to TORPEX, is connected to a turbomolecular pump. We need to control the pressure in the chamber constantly. If it rises too much, the emitter can be poisoned.

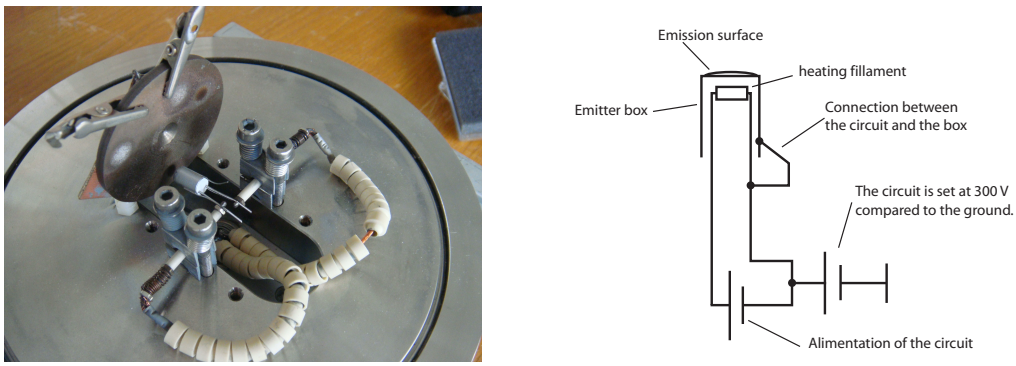

Figure 3.2: Photo and schema of a fast ions emitter mounted in the test vacuum chamber.

For the test, the current is set in the emitter. The box has a positive potential that is set by connecting one of the support struts with one of the filaments. No current will pass trough the box. The global circuit is set at a positive potential compared to the ground (Figure 3.7). In front of the emitter, a collector is put, about 2 cm from the emitter. The first time we heat the emitter we need to do it carefully and during a long time (about 8 hours), the next times we can do it faster (between 2 and 3 hours).

3.1.2 Test of the Fast Ions Emitters

This section shows the typical test results for a fast ions emitter. Here we have plotted different graphs; the heating power in function of the time, the current measured on the collector in function of the time and the current on the collector in function of the heating power.

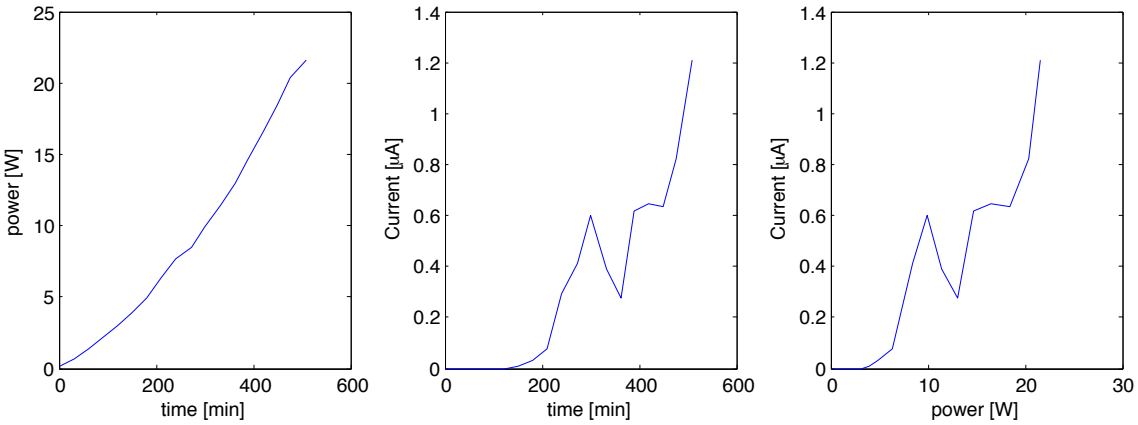

Figure 3.3: Results for the first test of an emitter.

A second test was made on the same emitter. The results are on the next figure, the figure takes the same axes as for the first test. And the results of the two tests are summarized on the following one, where the current on the collector is function of the heating power.

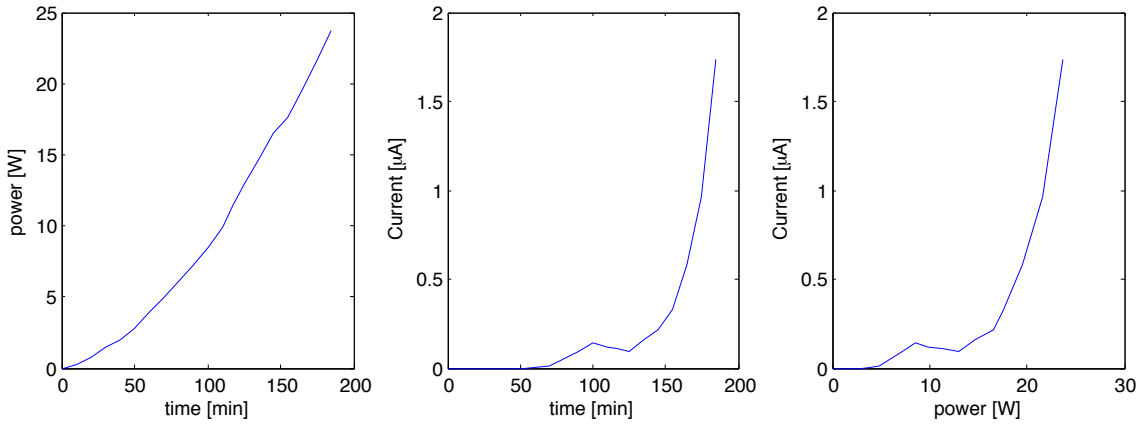

Figure 3.4: Results for the second test of the same emitter.

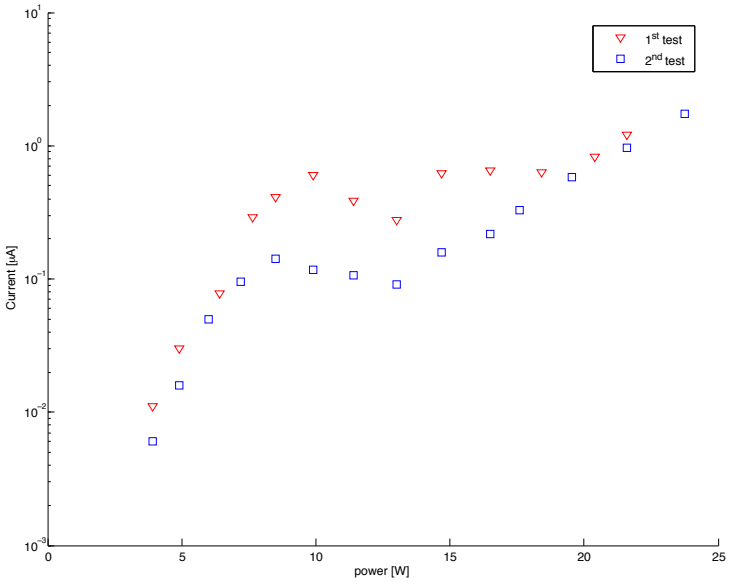

Figure 3.5: Current measured on the collector for the two tests of an emitter.

We have made two tests for every new emitter. We have tested an emitter that after been totally used has been sent to Hungary to be reloaded. The results of this test are on the following graph. On the graph, the current on the collector is in function of the heating power.

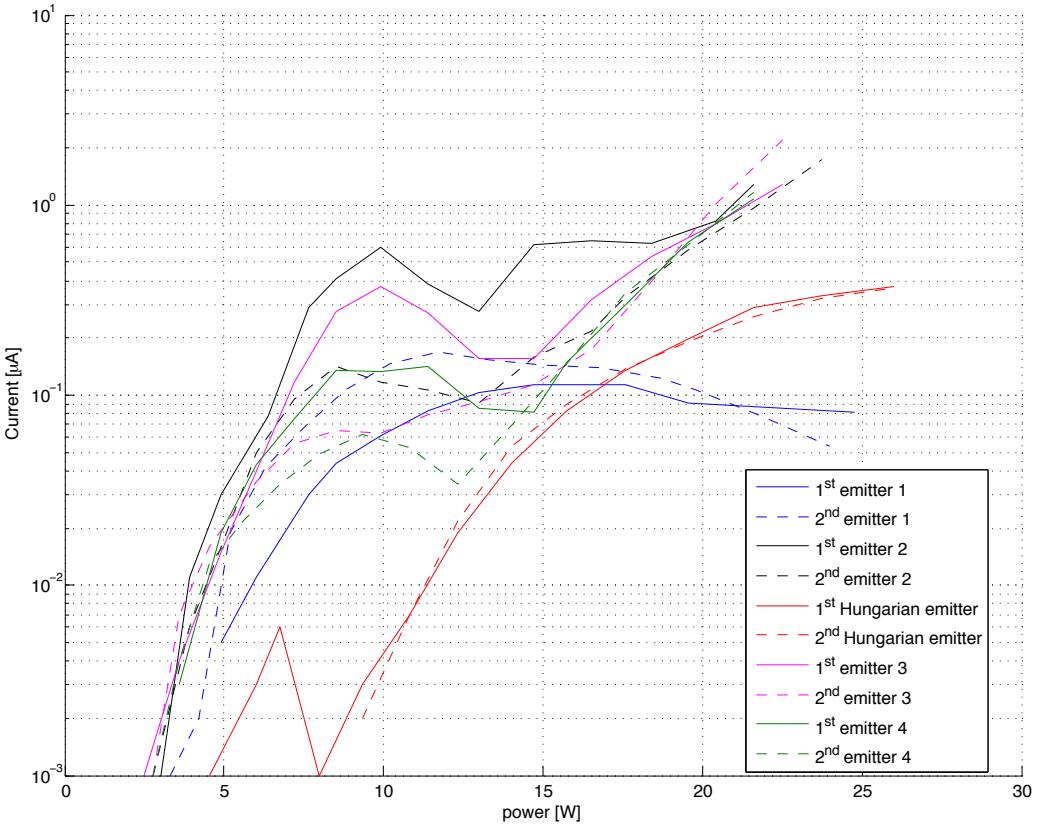

Figure 3.6: Results of the fast ions emitters.

We can see that the first emitter tested can't be used on TORPEX. The final current is too small and decreases when the heating current rises. We can see that for the other emitters, except the Hungarian one, the final current is higher than 1μA, we can then use them on TORPEX. When we heat them, the ions current first increase, it decreases a little bit between 10 and 15 W of heating, then it restarts to increase exponentially. This behavior, present on all the emitters exept the first we have tested, can be explained by the presence of impurities in the aluminosilicate lithium [6].

The exponential increase of the ions current is necessary to be sure that we are measuring an ions' current. When the temperature is high enough, about 16 W for the heating current, the emitter begins to emit light, it's at this moment that the emitter begins to emit a good ions current.

3.2 Fast Ion Source

The emitters that reach a good ions emission in the test chamber can be mounted on the source. The source has been designed to resist to the plasma condition, high temperature and vacuum, for the external part of the source. The internal part of the source has to resist not only to the operation in TORPEX but to the temperature of the emitter too, about 1100^{o}C. This source has been designed for [1].

The ion source consists of an ion emitter, mounted on a molybdenum support, put with two aligned grids in a boron nitride casing. Each grid has a support in molybdenum. They are isolated from the other grid and the emitter by a small piece in boron nitride (see following figures). The external grid will have the same potential as the plasma. The internal grid's potential will be negative and much higher than the electron temperature, to prevent electrons from reaching the emitter. The mesh size of the grid should be smaller than the Debye length to prevent penetration of plasma inside the source.

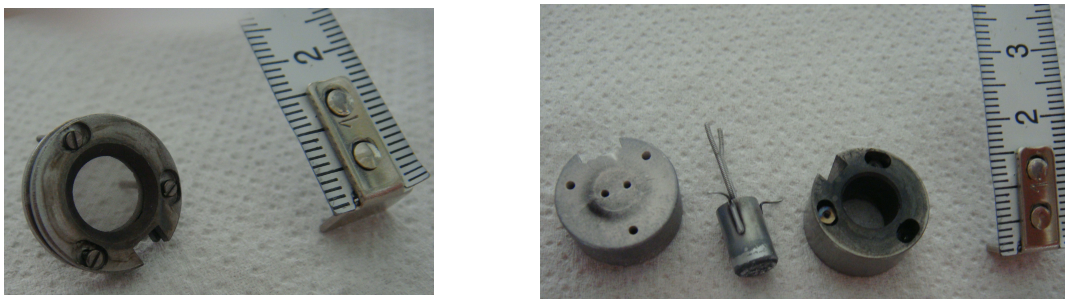

Figure 3.7: Source grid and emitter with the two support parts (scales in cm).

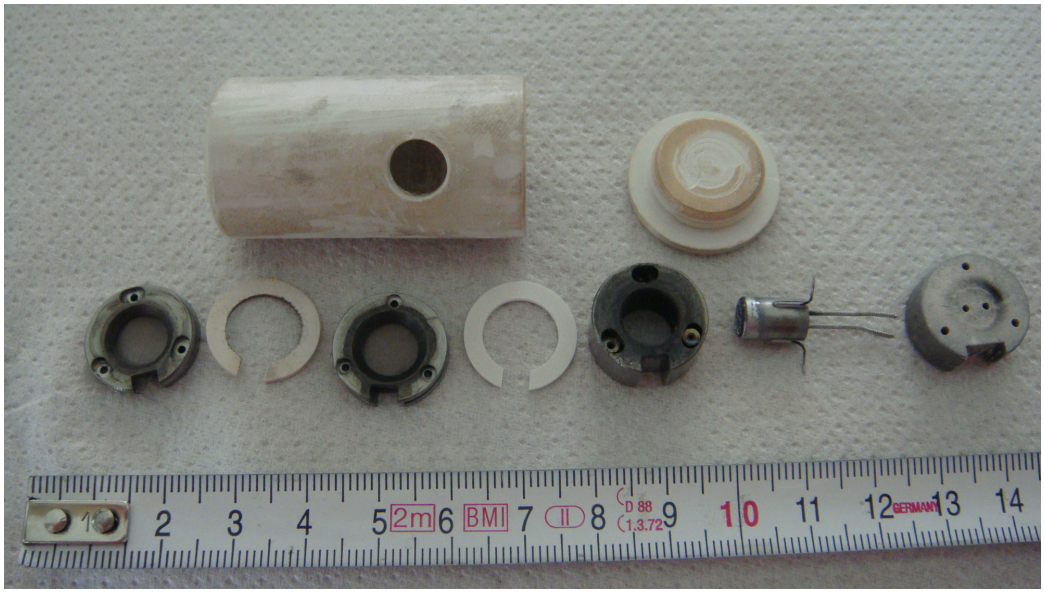

Figure 3.8: Main parts of the fast ion source (from left to right: external grid, isolation, internal grid, isolation, first emitter support, emitter, second emitter support, scale in cm).

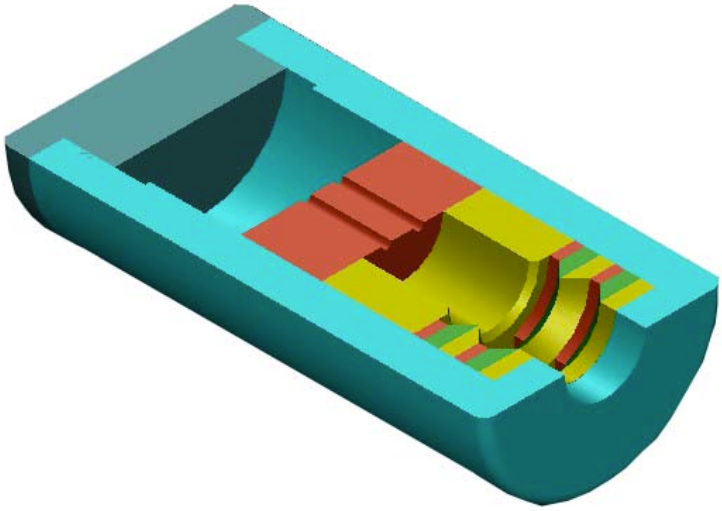

Figure 3.9: The schematics of the source, without emitter.

The source is glued with a ceramic tube with the glue "Resbond 989".

This glue can resists to a temperature up to 1600^{o}C. The ceramic tube is screwed to a stainless steel tube which is connected on the TORPEX vessel. In the ceramic tube, cable are isolated from each other with smaller ceramics tubes. In the stainless steel tube, this isolation is made with shrinkable tubing. A connector at the end of the stainless steel tube is used to connect the grids and the emitter. All this material is mounted on a 2D poloidal moving system, designed to be plugged into the TORPEX. This moving system is equipped with differential pumping and provides an angular excursion of up to 70^o. With this system, we will be able to choose the position of the source.

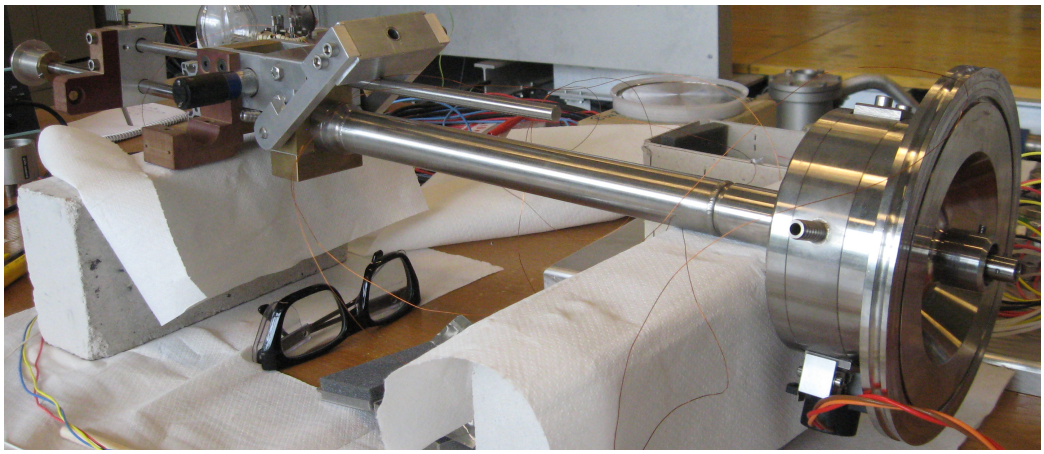

Figure 3.10: Moving system and inox tube of the source.

Before mounting the source on TORPEX, it's possible to test it in the small vacuum vessel. On the following figure, we can see the result of this test for the emitter used on TORPEX. This time, the external grid play the role of collector. We measure a part of the ions current, the other part go out of the source and is the ions beam that we will use in TORPEX to investigate the ions dynamics in plasma.

When an emitter mounted on the source pass the test in the small vacuum vessel, it can be mounted on TORPEX. We can see a big difference between the test of the source in the small vacuum chamber and the heating in TORPEX. The emission of ions is one order bigger in the TORPEX than in the test vacuum chamber. An explanation can be the different environments. The pressure and the nature of the gas is different in TORPEX. After the

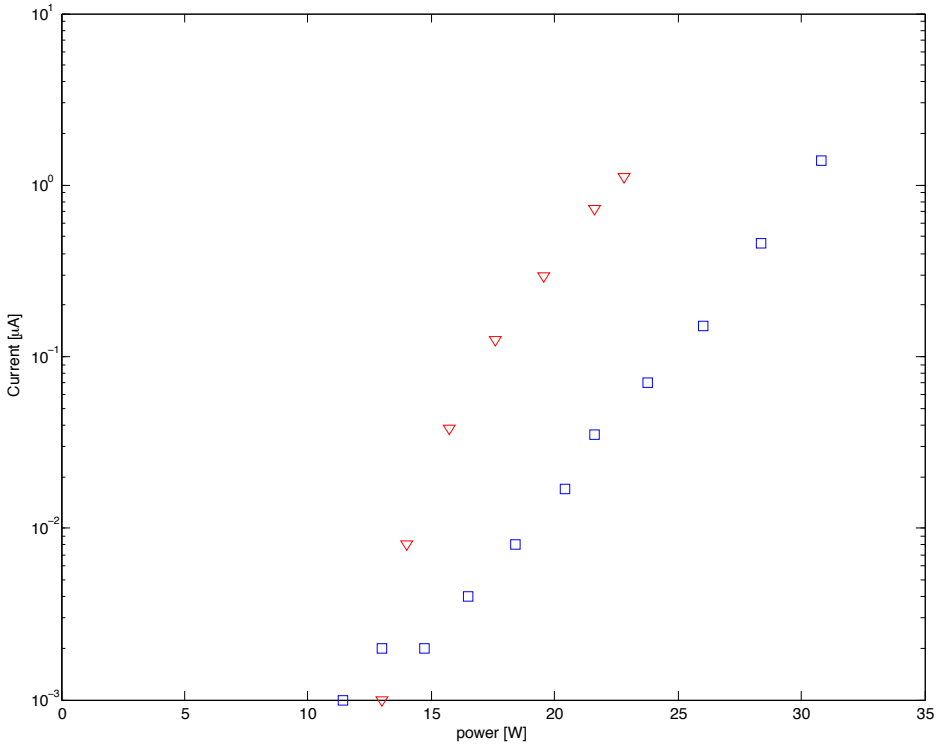

Figure 3.11: Results of two different heatings of the emitter mounted on the source. First in the vacuum chamber (blue), then in the TORPEX (red).

test of the emitter, without the source, it has stay for a while at atmospheric pressure. Then we have mounted it on the source, test it in the small vacuum chamber and then directly mounted it on TORPEX. We can't know if impurity has been put on the source between the firsts tests an the moment it has been mounted on the source. This impurity have maybe been removed during the heating in the vacuum chamber which offer the possibility to have a higher emission for the next heating in TORPEX.

Chapter 4

Double Gridded Energy Analyzer

As seen in the previous section, the fast ions beam is very low. We then have to use a probe which will be able to make the difference between the fast ions and the plasma. It must be designed to resist to the plasma and the vacuum. We have used the double gridded energy analyzer developed for [1].

4.1 Synchronous Detection

The noise in the plasma will be higher than the fast ion signal. To be able to make the difference between the signal and the noise, the beam is modulated. To modulate the beam, we modulate the potential on the fast ion emitter. This potential varies between 0 (no ions emitted) and a chosen potential. This potential affects the energy of ions out of the source. In the following picture, we can see the modulation in red (it varies between 0 and 300 volts) and the signal measured on the probe.

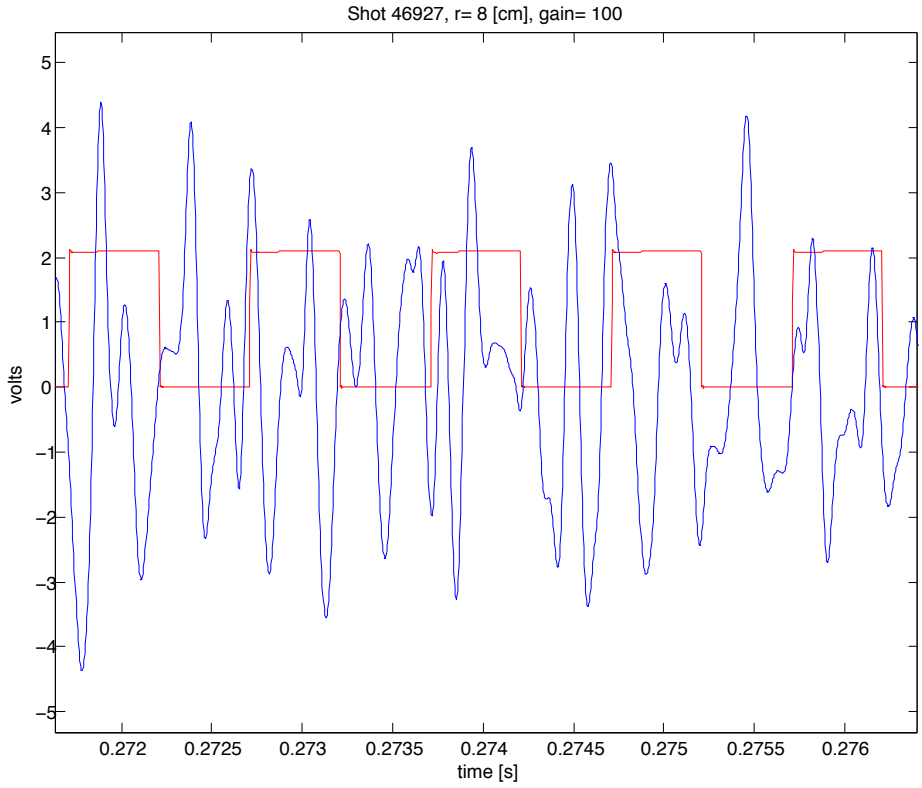

Figure 4.1: Signal measured on the probe and modulation of the emitter.

The problem now resides in extracting the ions signal from the noise. This is done by using synchronous detection. Let's consider a sinusoidal signal embedded in noise.

$$Sig = Sig_0 \cdot cos(\omega t + \psi_s) + U_{noise} \tag{4.1}$$

Sig_0 is the power of the signal, ω is the modulation frequency, ψ_s the relative phase of the signal and U_{noise} the power of the noise. The reference signal can be express as:

$$Ref = Ref_0 \cdot cos(\omega t + \psi_r) \tag{4.2}$$

If we multiply this signal by the reference, we obtain:

$$y_1 = Sig \cdot Ref = Sig_0 \cdot Ref_0 \cdot cos(\omega t + \psi_s) \cdot cos(\omega t + \psi_r) \tag{4.3}$$

Plus a component with the noise which will be filter with a low pass filter. With the trigonometric identity: $cos\theta \cdot cos\delta = \frac{cos(\theta-\delta)+cos(\theta+\delta)}{2}$:

$$y_1 = \frac{1}{2} Sig_0 Ref_0 \cdot [cos(\psi_s - \psi_r) + cos(2\omega t + \psi_s + \psi_r)] \tag{4.4}$$

Here, the low pass filter will filter the component with high frequency like the noise and the component with the $2\omega t$. We then have:

$$y_1 \approx \frac{1}{2} Sig_0 Ref_0 \cdot cos(\psi_s - \psi_r) = \frac{1}{2} Sig_0 Ref_0 \cdot cos(\Delta\psi) \tag{4.5}$$

Imposing a phase shift of $\frac{\pi}{2}$ on the reference and doing the same treatment leads to:

$$y_2 \approx \frac{1}{2} Sig_0 Ref_0 \cdot sin(\Delta\psi) \tag{4.6}$$

We can now have R:

$$R = y_1 + i \cdot y_2 = \frac{1}{2} Sig_0 Ref_0 \left[cos(\Delta\psi) + i \cdot sin(\Delta\psi)\right] = \frac{1}{2} Sig_0 Ref_0 \cdot e^{i\Delta\psi} \tag{4.7}$$

We are now able to find the power of the signal:

$$Sig_0 = \frac{2|R|}{Ref_0} \tag{4.8}$$

The first goal of this diploma was to use this method with matlab©, using the gross traces, calculating the fast ions' current numerically. But the problems with the probes lead us to integrate this method directly in the hardware and to develop a devices which does this (see section 4.3.1).

4.2 Previous Setup

The double gridded energy analyzer is made of two symmetric part, each made of two aligned grids and a collector. The external grid is set at the plasma potential to minimize the plasma perturbation. The internal grid's potential will be negative and much higher than the electron temperature, to prevent electrons from reaching the collector. When we use this setup, one gridded energy analyzer (GEA) will measures the fast ions beam together with the plasma background, while the other GEA measures only the plasma background. We then take the difference between both signals to rebuild the fast ions signal.

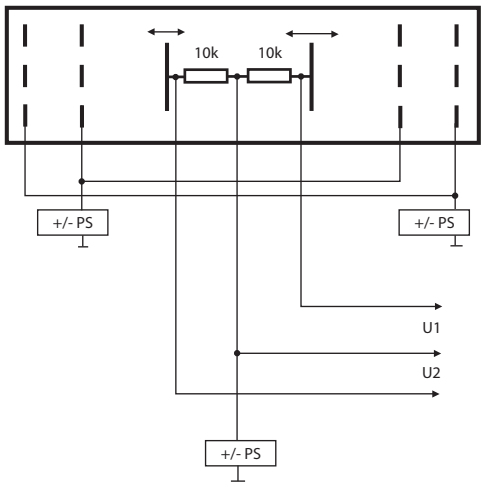

Figure 4.2: Connection of the old probe setup.

4.3 New Setup

After using the previous setup, developed for [1], we realized that some problems are present on the hardware. A loop mass start at the source and goes to the detector. This provides the spikes we can see on the followings figures (plotted in blue).

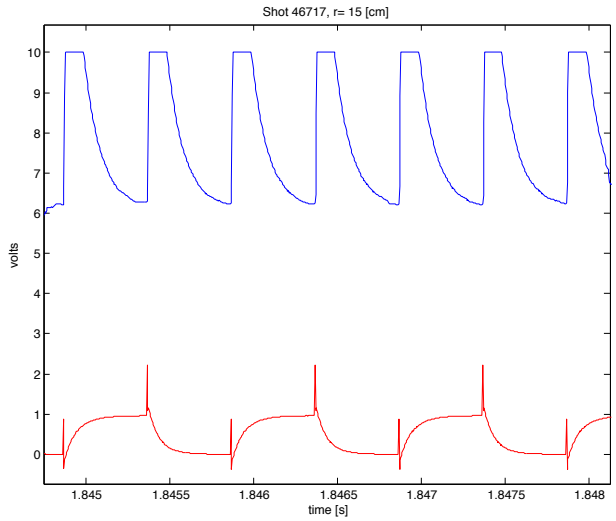

Figure 4.3: Signal on the detector (blue) and referential modulation (red) without plasma.

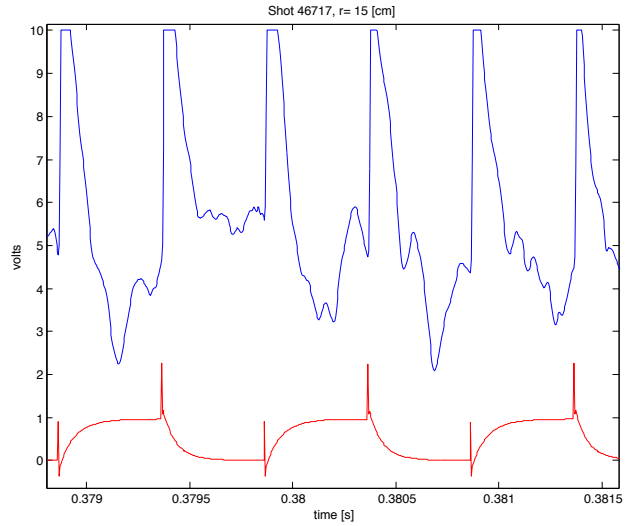

Figure 4.4: Signal on the detector (blue) and referential modulation (red) with plasma.

As we can see on figure 4.3, the difference between the signal with the emission and without can be very small compared to the size of the signal.

We can see peaks on the referential signal, it's hard to know how it affects the ions emission in the source.

We also realized that it's hard to find the position of the beam because it moves when the magnetic field is swhich on and when the plasma is present. We then decided to change the way the detector works. We decided to design a setup which will extract the ions signal (on the detector) before acquisition. With this device we won't need a very fast acquisition, 250 KHz for the previous setup, 1 KHz is enough. We first changed the connection in the GEA and just after the connector. The plan of the new connections is on the following picture.

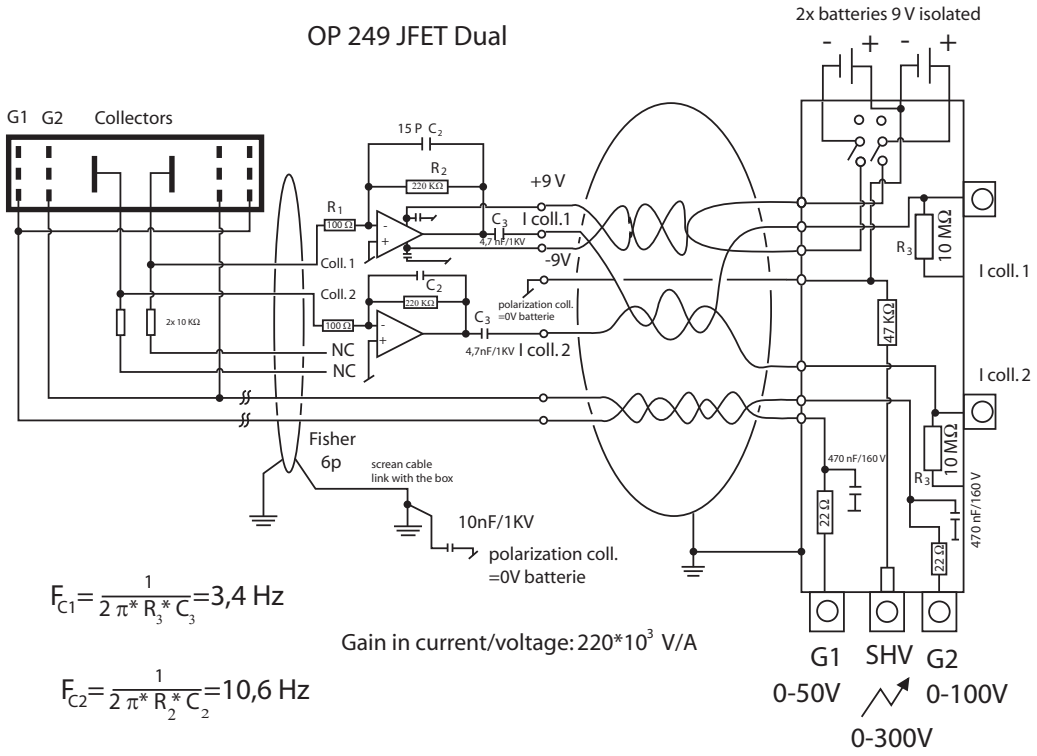

Figure 4.5: Connection of the new probe setup.

The signal is then sent to the lock-in device which provides a filter based on the modulation of the source (see 4.3.1). With this system, we are now

directly able to measure the ions signal, without the plasma background, after the lock-in, but we don't make the acquisition of the primary signal. To use it in a better way we have developed a new technique of scanning in TORPEX. For the previous diagnostics, we were doing a plasma shot for every position. Then move the probe and do an other shot. It can take hours for a single profile. And the size of the signal acquired (with an acquisition frequency of 250 KHz) takes a lot of place in the data bases. By the time we use a smaller acquisition frequency, we are able to do longer shots. And are able to move the probes during the shots. It makes it possible to do a complete profile in less than 10 minutes.

4.3.1 Look-in Device

Two signals are in the entrance of the device. The reference (a ttl signal) and the signal detected by the probe. The ttl signal is used on a swhich to charge a capacitor in phase with the signal (see next figure). When the reference is positive, the signal is positive and charges the capacitor. When the reference is negative, it charges the capacitor with a negative signal but in the opposite direction, that finally charges the capacitor in the same direction as before. If we do this for a long time, with a big time constant of the RC, the charge of the capacitor will be proportional to the average of the initial signal.

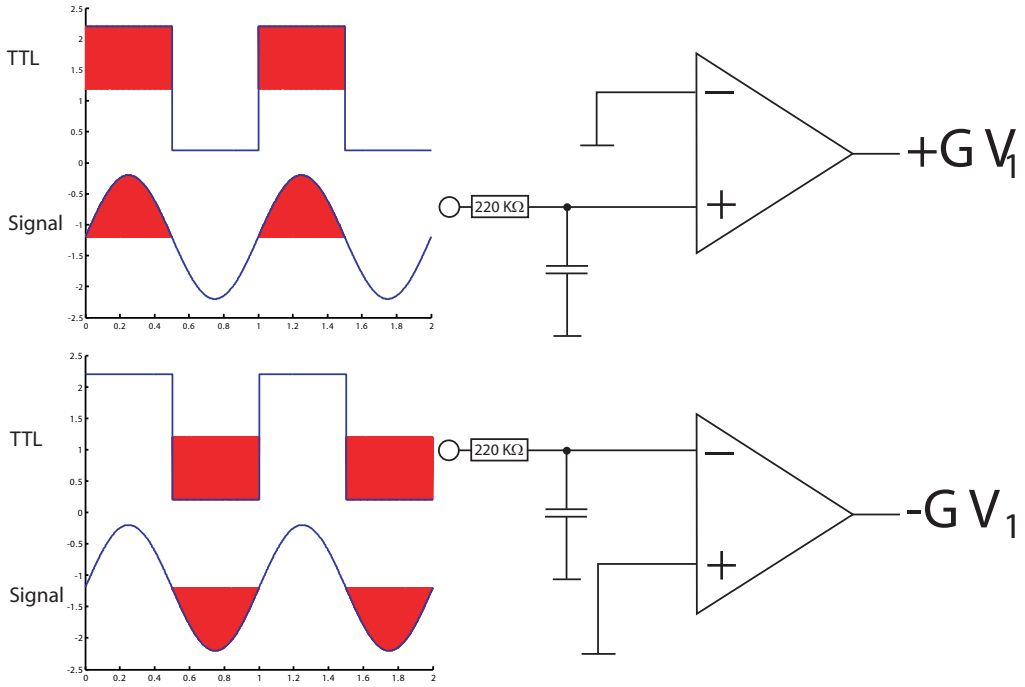

Figure 4.6: Charge sent to the capacitor in the lock-in.

After that, a differential amplifier gives the potential difference between the two sides of the capacitor. A classic RC works as a low pass filter. When it's used with a swhich like in the lock-in device, the low pass filter is moved at the modulation frequency, and is repeated at the odd harmonics.

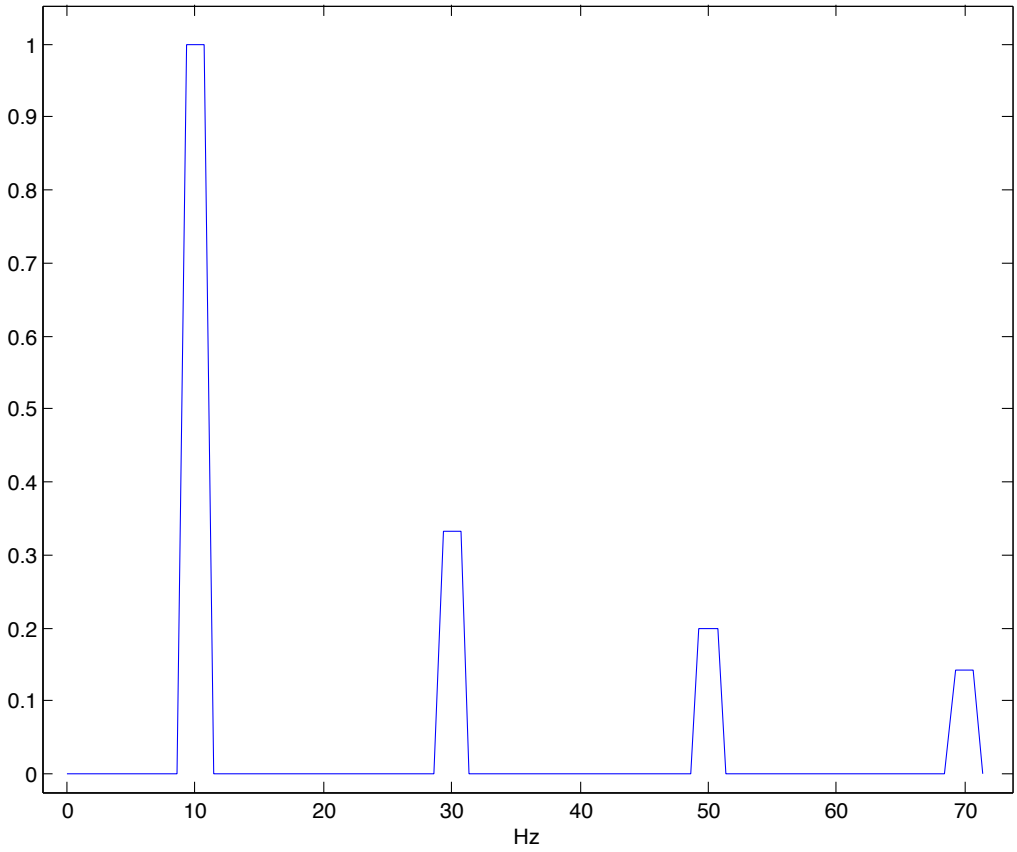

Figure 4.7: Filter in frequency in the lock-in device. Here with a modulation of 10 Hz.

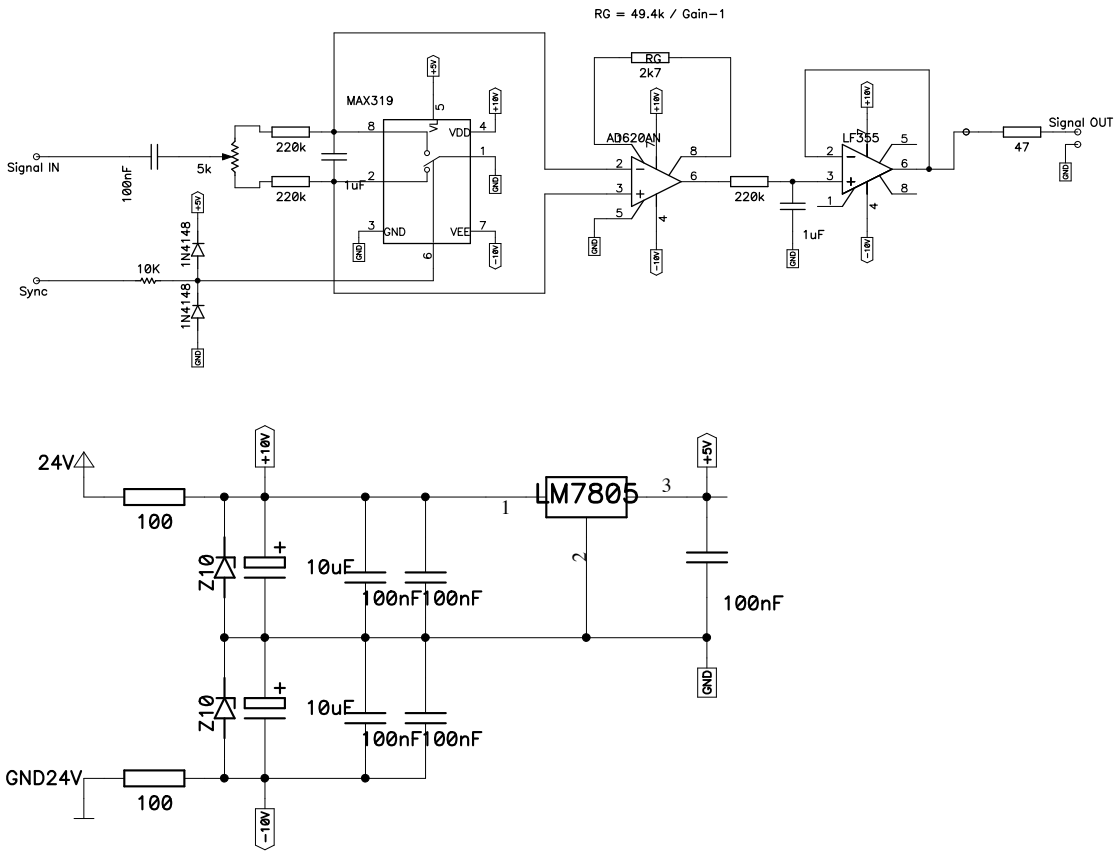

Figure 4.8: Connections in the lock-in device

The last amplifier is there to filter the low frequency.

Calibration of the Lock-in

We have chosen a big time constant for the RC so the tension at the sides will be an integration over a long time. This time constant influence the low pass filter. $\omega_0 = \frac{1}{RC}$, $\tau = RC = 220ms$, $\omega = \frac{1}{220ms} = 5rad/s$ so we have a cut-off frequency of $f = \frac{\omega}{2\pi} = 0.7Hz$. This low pass filter decrease of 20 dB/dec.
The choice of the modulation frequency is important, we need to avoid a recovery of the band pass and an harmonic of 50 Hz, provides by the alimentation. So we decided to use a modulation of 70.9 Hz.

Data Acquisition

As said before, with the lock-in device, we are able to do a complete profile in less than 10 minutes. This time depends on the noise. Without plasma and without magnetic field, the noise is low enough to acquire data during 300 ms and have a good profile. In a plasma shot of 5 min we can do a complete scan. When we had the magnetic field, and even more when we had the plasma, we need a longer time to have a good average. In the following graphs, we can see how the mean of the signal out of the lock-in device evolves when we take longer shots.

We made this test without ions signal, this means that the results must be 0 out of the lock-in. We can see that it's not the case. We have plotted here the absolute value of the average out of the lock-in device. This average is plotted in function of the time over which we have averaged. We have made this at the positions; +3 cm, -1 cm and -5 cm. This means that we are always more in the plasma region. We can see that the deeper in the plasma we are, more time we need to decrease the average. We then need to choose the length we need to make the acquisition.

Without plasma and without magnetic field, an acquisition time of 300 ms is long enough. Without plasma but with the magnetic field, we decided the measure the signal over 15 s, and over 35 s with the plasma. This decision influences the length of the shots and the total acquisition time for the profile. The quantity of data acquired during a complete shot is limited. With the times we have chosen, we are only able to scan a big region without plasma and without magnetic field. When we add the magnetic field or the

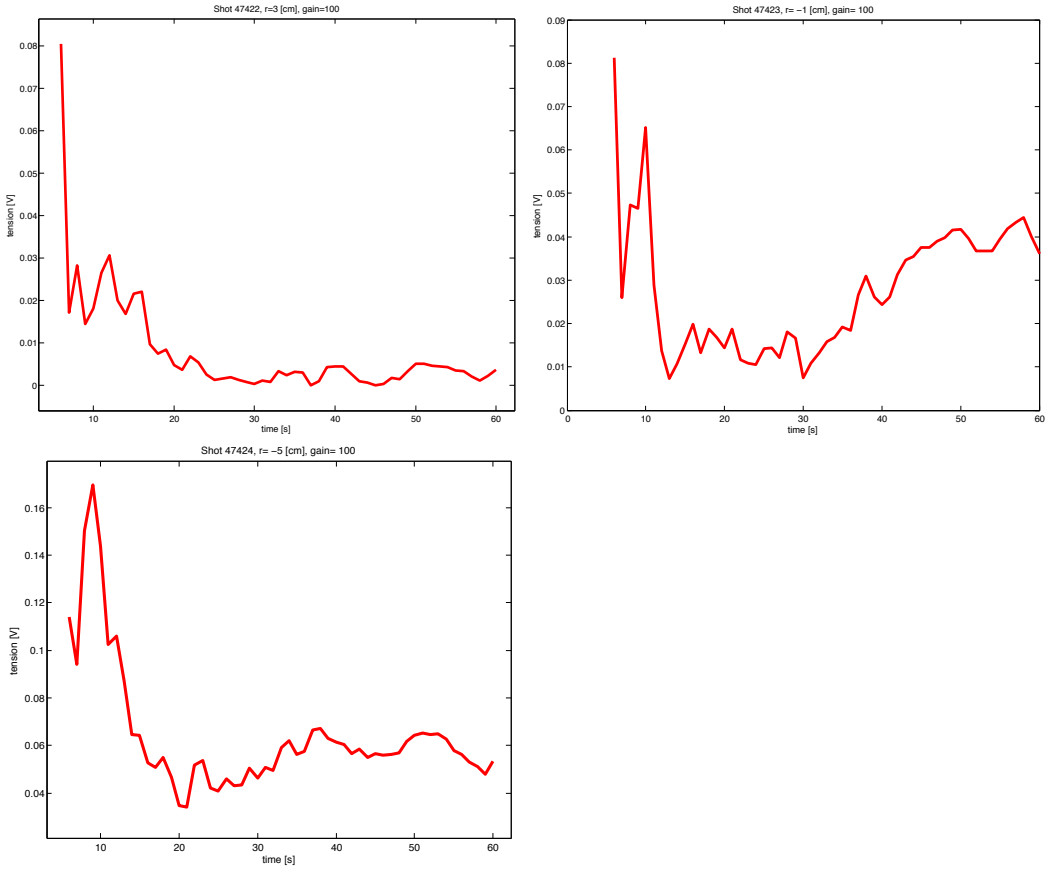

Figure 4.9: Average of the lock-in in function of the averaging time

plasma, we need to do more shots for one profile. One shot is only a scan in translation of the probe, then a rotation of the detector is necessary before the next shot.

4.4 Moving System

The detector has the same moving system as the source. It is glued to a ceramic tube with liquid ceramics, this tube is screw to a stainless steel tube which is attached to a moving system like the one described in section 3.2. The moving system is plug on TORPEX on the LFS. Outside of TORPEX, two motors are connected to the system, one for the translation and one for the vertical rotation. This system is formed of three types of connection, the

motor's power supply, the potentiometer and the security. For the rest of this diploma, when we are talking about a positive inclination angle for the probe this means that the detector is on the upper part of TORPEX.

The power supply will activate the motor in one direction or the other, whether we want to introduce or take out the probe, for the translation. With the other we can rotate the stainless steel tube up or down. The potentiometers are here to know where the probe is. The voltage we measure on the potentiometer is proportional to the translation of the tube or its rotation. We then only need to calibrate and convert it to cm or degrees. The position of the probe can be, with this system, directly acquired in the data bases. The error margin in the acquisition of the position is 0.3^o in rotation and 0.5 cm in the translation.

Chapter 5

Experimental Results

We present here the profiles measured on TORPEX. As said in chapter 4 the detector is attached to TORPEX on the low field side. If we put the referential in the center of a poloidal plane of TORPEX, we will keep this choice of referential for the rest of this diploma. The probe is attached at the position (20,0). We can see this choice of referential on the figure 2.4. This means 20 cm from the center of the poloidal plane. We have chosen, to make the profiles, steps for the detector of 3 cm for the translation of the detector and 5^o for its rotation. We can see on the next figure the point where we make the average of the ion signal out of the lock-in device. We can see that the resolution decreases when the distance between the detector and the moving system increases.

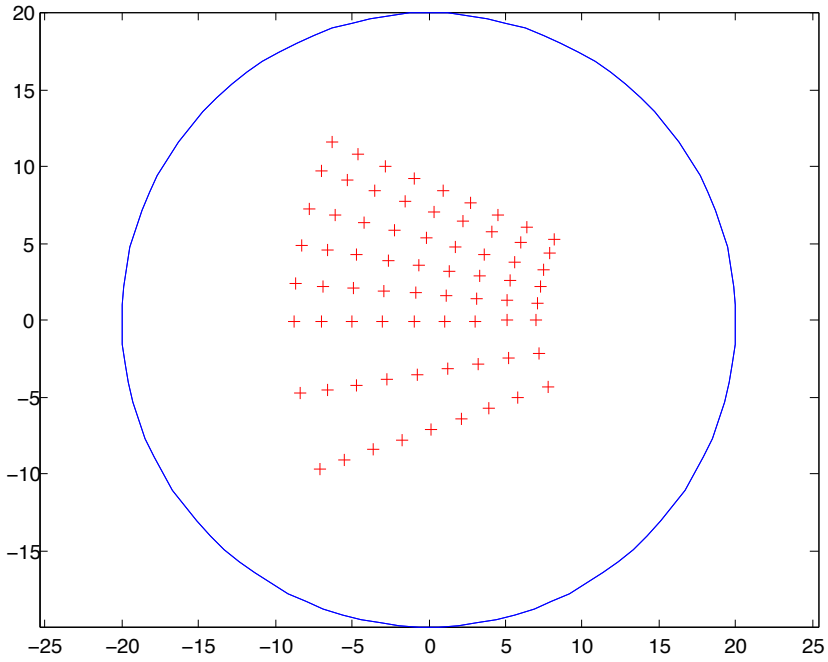

Figure 5.1: Typical scanning points.

It was very hard to be able to do measurements. The main problem resides in the source. We installed 3 different emitters in the source. All of them have reached more than $1\mu A$ during the tests in the small vacuum chamber. We weren't able to do measurement with the first on, because problems of short circuit appeared, first between the different cable, then between filaments and the stainless steel tube. It's at this moment that we decided to use the shrinkable tubing to isolate the cable. To increase our chances to do enough measures without changing the emitter, we decided to change it. The test with the second emitter mounted in the source is presented on the figure 3.11. This emitter passed the tests, we then decided to do measurements with the previous setup. After a series of shots, we discovered the problems and change the setup for the new one with the lock-in device (presented in chapter 4). We have heated this emitter 8 times in the source. Some times juste to test it, like in the small vacuum chamber or to test the new setup, and some times to make fast ions measures. After the 8^{th} heating, the current measured on the external grid seems to decrease. We then decided to change the emitter. The first time we heated the source, the current on the external grid didn't reach $0.2\mu A$. The second time the current

was negative. It seems that this emitter wasn't emitting ions. These tests took place on the 3^{rd} and the 7^{th} June. Since the deadline to render this diploma was the 25^{th}, we decide to stop the experiment. However, we have made some tests with the last emitter to see how was the detector behavior in this condition.

5.1 Experiments Without Plasma and Without Magnetic Field

With the second emitter mounted on the source, we made profiles in TORPEX with two different potential on the emitter, 300 and 500 V. This means that the particles have energies of 300 and 500 eV. The potential on the internal grid is always -100 V. For the profile with 300 V, the source was at the position (-1,0), we then moved it to (8,0) for all the other profile, at 500 V and with the magnetic field or the plasma.

Before presenting the profiles, we present here the traces measured out of the lock-in device. On the following graph, we have the position of the probe.

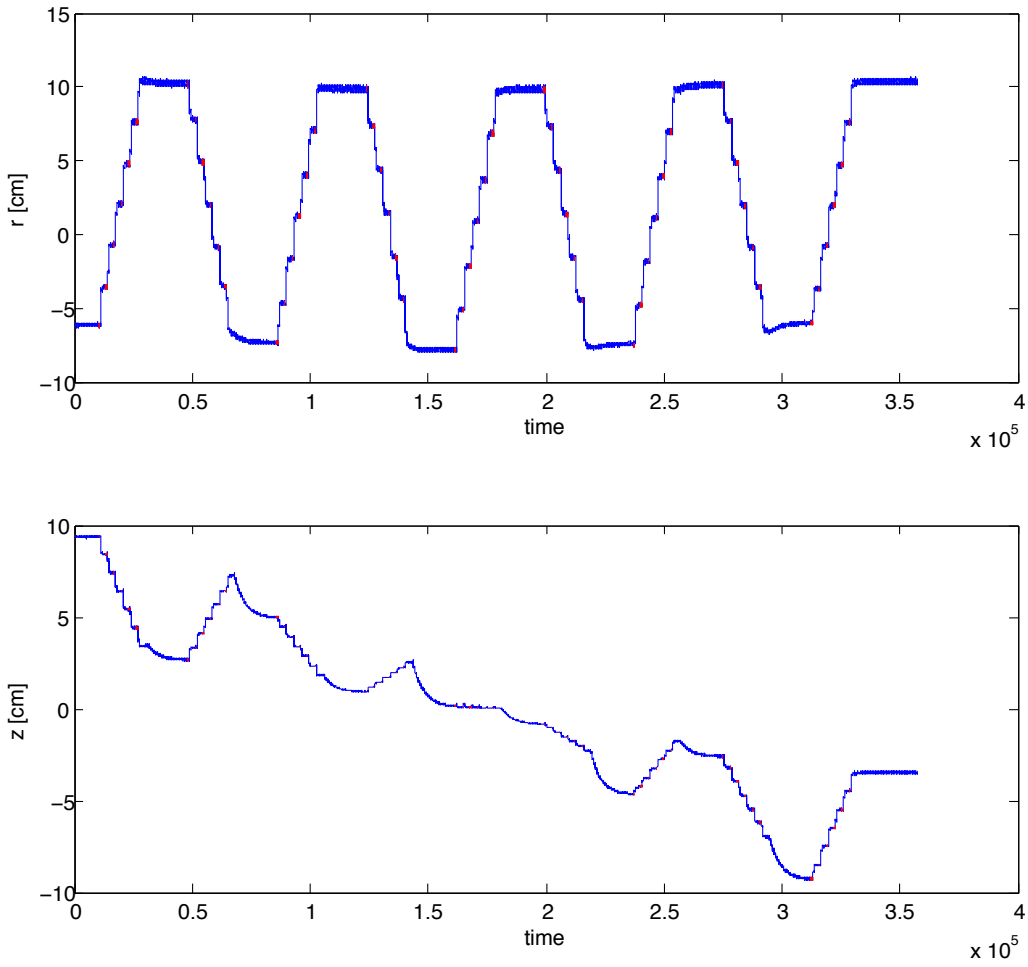

Figure 5.2: Position of the detector.

The horizontal axis shows the time (in acquisition points, one point every $10^{-3}s$). The next figure shows the voltage measured out of the lock-in device. The horizontal axis is the same and the vertical is the voltage out of the lock-in device.

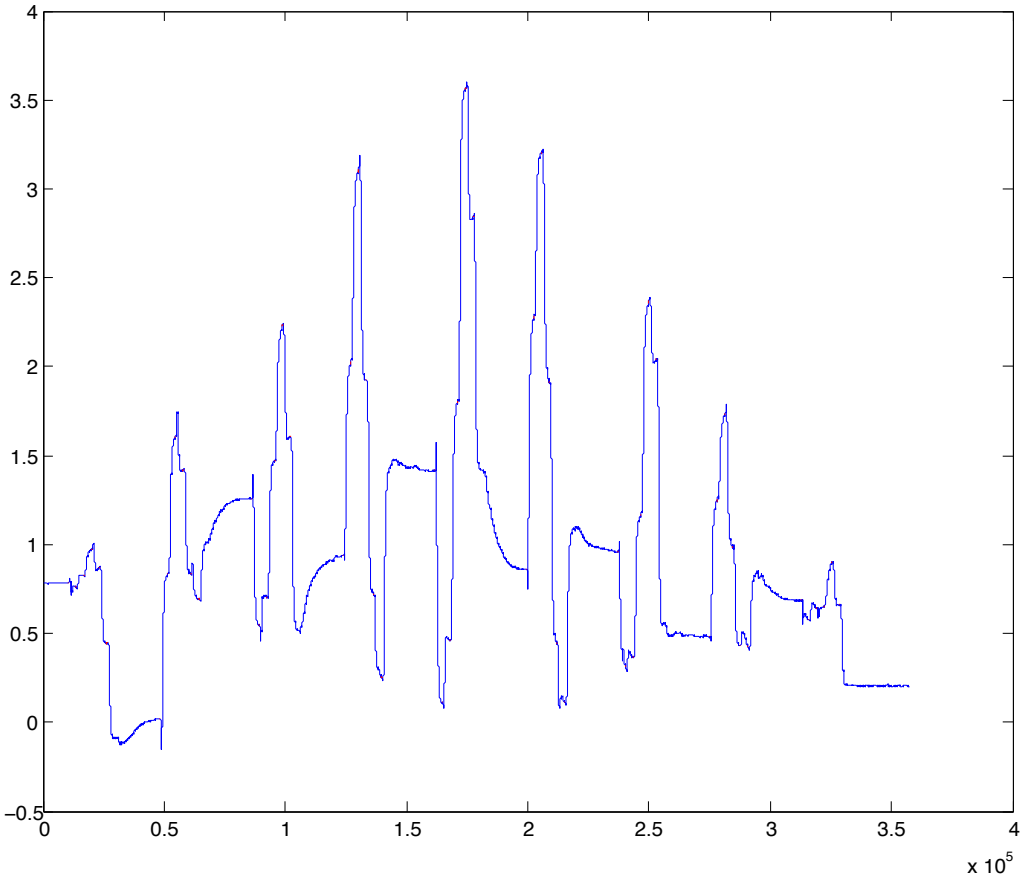

Figure 5.3: Voltage out of the lock-in device.

5.1.1 Profile With 300 eV

Here is the profile measured with the GEA and treated with the lock-in device.

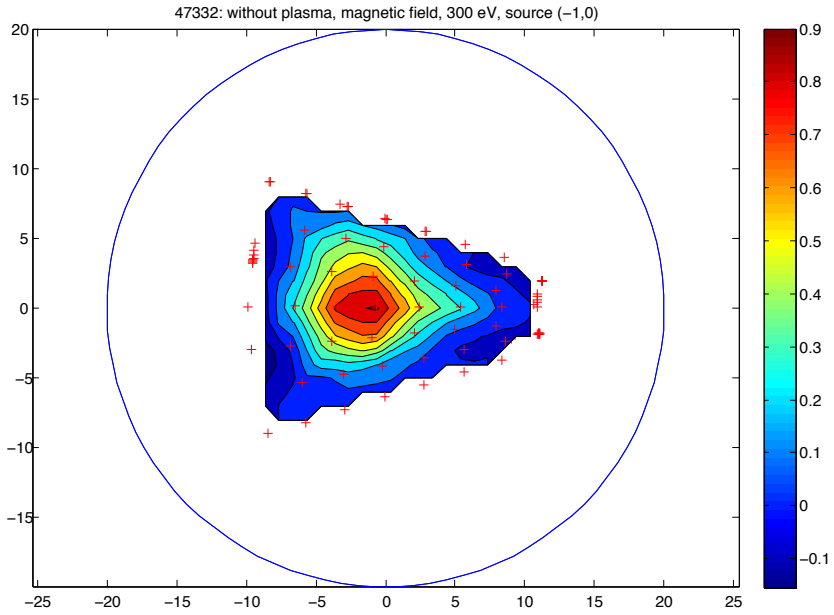

Figure 5.4: Ions' current on the detector, energy's ions of 300 eV.

The current measured on the source's external grid is $1.046\mu A$. Knowing the resolution of the profile on figure 5.4, the different gain in the circuit after the detector and the size of the collector in the probe, we can calculate the total current measured, which is $0.2766\mu A$. We need to remember that the ions' current measured on the source's external grid is the current which doesn't go out of the source. Between the source and the detector, part of the ions might be neutralized. An other part of the ions will be capture by the external and internal grids of the detector. This can explain the different between the current on the source's external grid and the current calculated, based on the signal after the lock-in device.

On the following graph, we have a vertical and a horizontal cut of the profile run through the maximum of the profile (measured at (-0.6,0.1)).

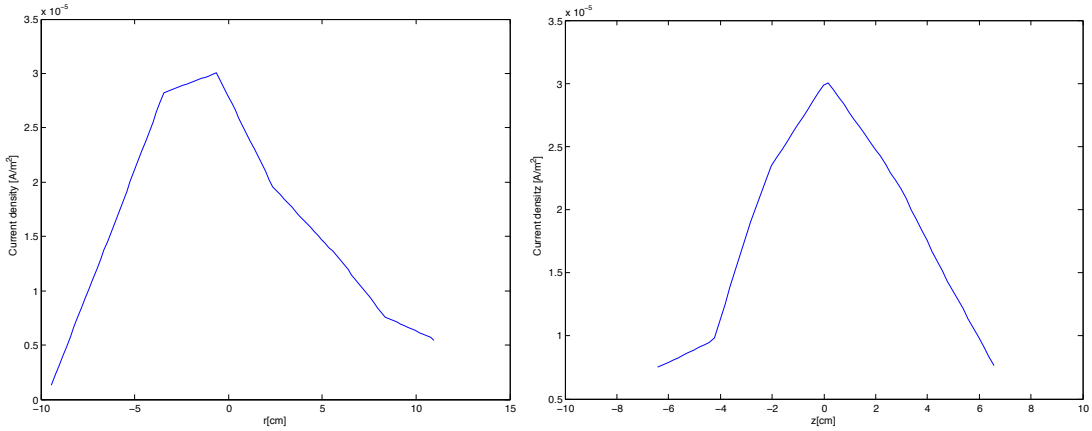

Figure 5.5: Horizontal and vertical cut of the ions' beam profile.

On the vertical axis, the width at half height is about 8 cm and 11 cm on the horizontal axis. This difference can be explain by the geometry of the experience and the assembly of the source.

5.1.2 Profile With 500 eV

We have on the following picture the profile measured for the ion's beam of 500 eV.

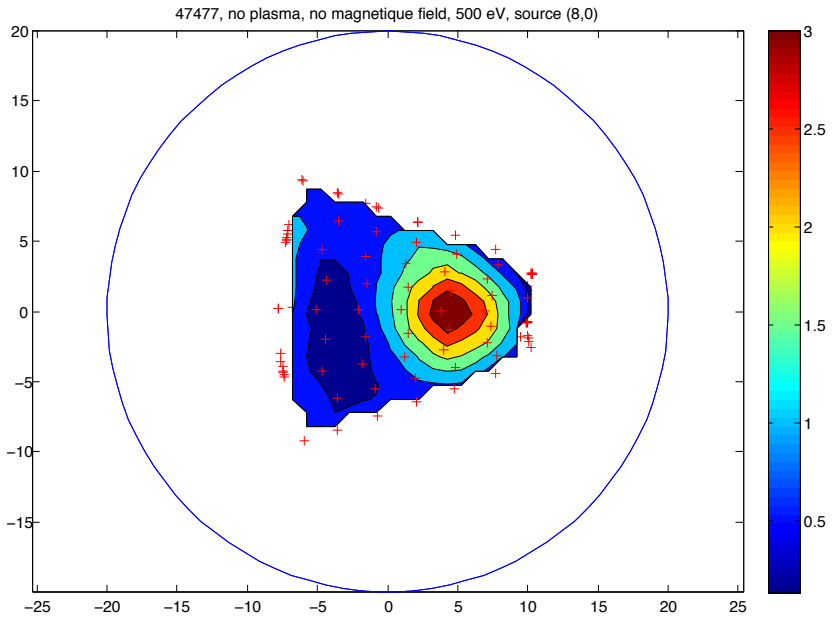

Figure 5.6: Ions' current on the detector, energy's ions of 500 eV.

This time, the current on the source's external grid was $4.3\mu A$ and the total current calculated in the same way as in 5.1.1 is $0.6156\mu A$.

On the following graph, we have a vertical and a horizontal cut of the profile run through the maximum of the profile (measured at (3.8,0)).

We can see that the beam seems to be isotropic, the width at half height is about 7 cm on the horizontal axis and 7.5 cm on the vertical axis. These results are used in chapter 6 for a calibration simulation.

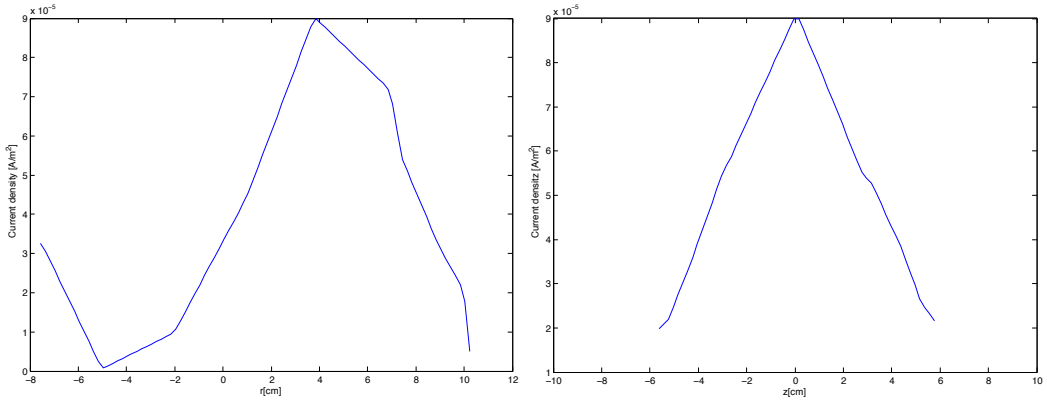

Figure 5.7: Horizontal and vertical cut of the ions' beam profile.

5.1.3 Profiles Measured with the 3^{rd} Emitter

On the followings graphs we can see the profiles measured with the 3^{rd} emitter.

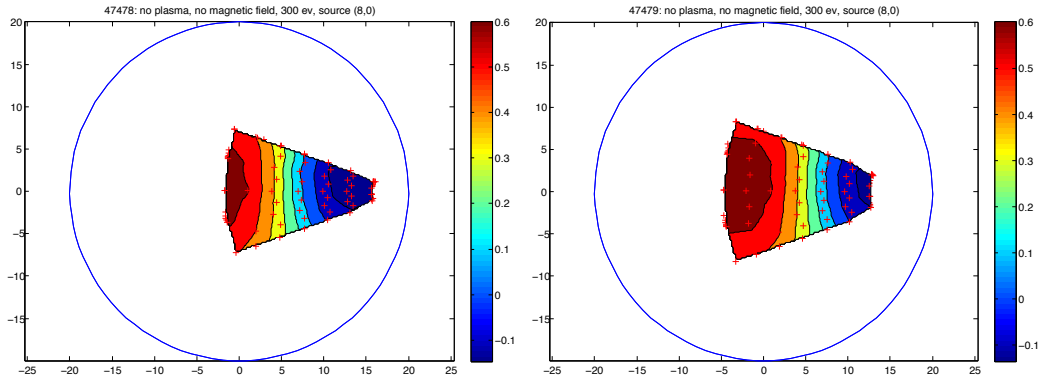

Figure 5.8: First profiles with the 3^{rd} emitter.

For these profiles, the ions' current on the source's external grid was $0.15\mu A$. On the next graphs, we have the profiles made when the current on the source's external grid was negative.

We discuss this strange behavior in the chapter 6 which seems to be a capacitive effect.

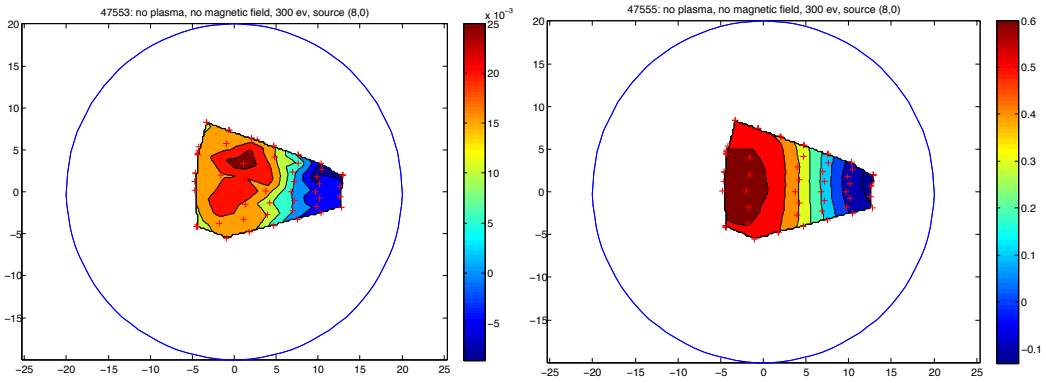

Figure 5.9: Second profiles with the 3^{rd} emitter.

5.2 Experiments Without Plasma and With the Magnetic Field

We present here the profiles with the magnetic field but without plasma. The ions' energies is 300 and 500 eV. The source is at the position (8,0).

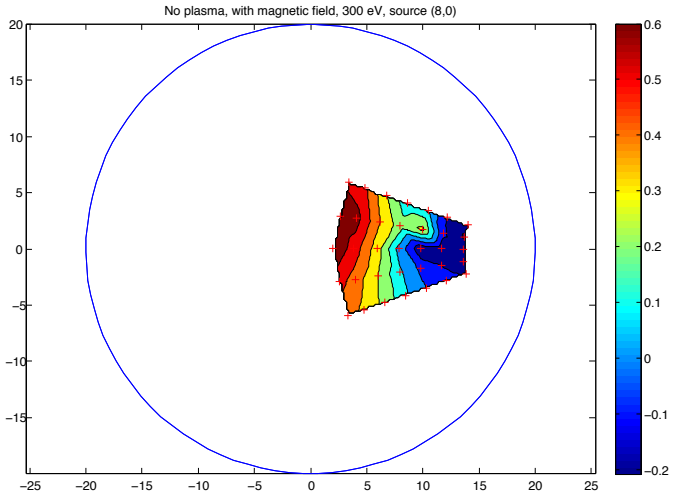

Figure 5.10: Ions' current on the detector, energy's ions of 300 eV.

It seems that the ions current is the same for both, but the current measured on the source's external grid isn't the same for 300 and 500 eV, between

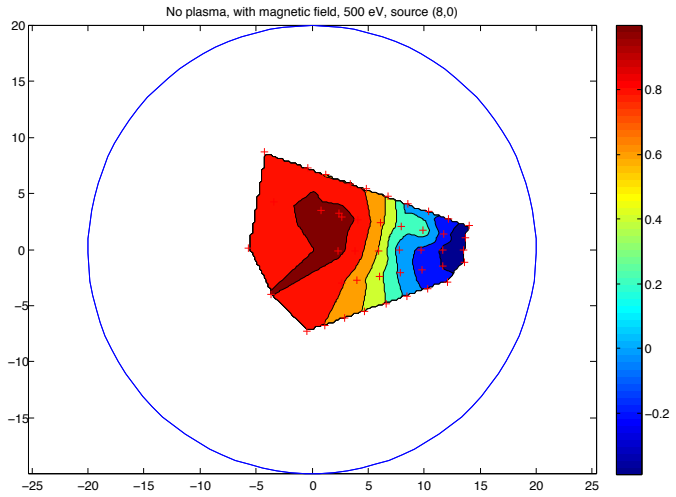

Figure 5.11: Ions' current on the detector, energy's ions of 500 eV.

0.6 and 1.2 μA for 300 eV and between 4.6 and 5 μA for 500 eV. The emitter is the same as the one used for the profiles 5.4 and 5.6. We have a very big difference between the profile without and with the magnetics field. As said in chapter 1, a particle in a magnetic field will have a cyclotron movement around the magnetics line and suffer a drift. This means that the beam should be smaller with the magnetic field and a little bit on the left and upper from the initial position. We clearly don't have this. We think that it's the same effect as we have seen for the profile without magnetic field, with the 3^{rd} emitter.

5.3 Experiments With Plasma

Although tests with the magnetic field with the 2^{nd} emitter weren't good, we decided to measure the ions' current in plasma conditions. The results are presented in this section.

5.3.1 Profile With 300 eV

Here is the ions' current measured with the detector.

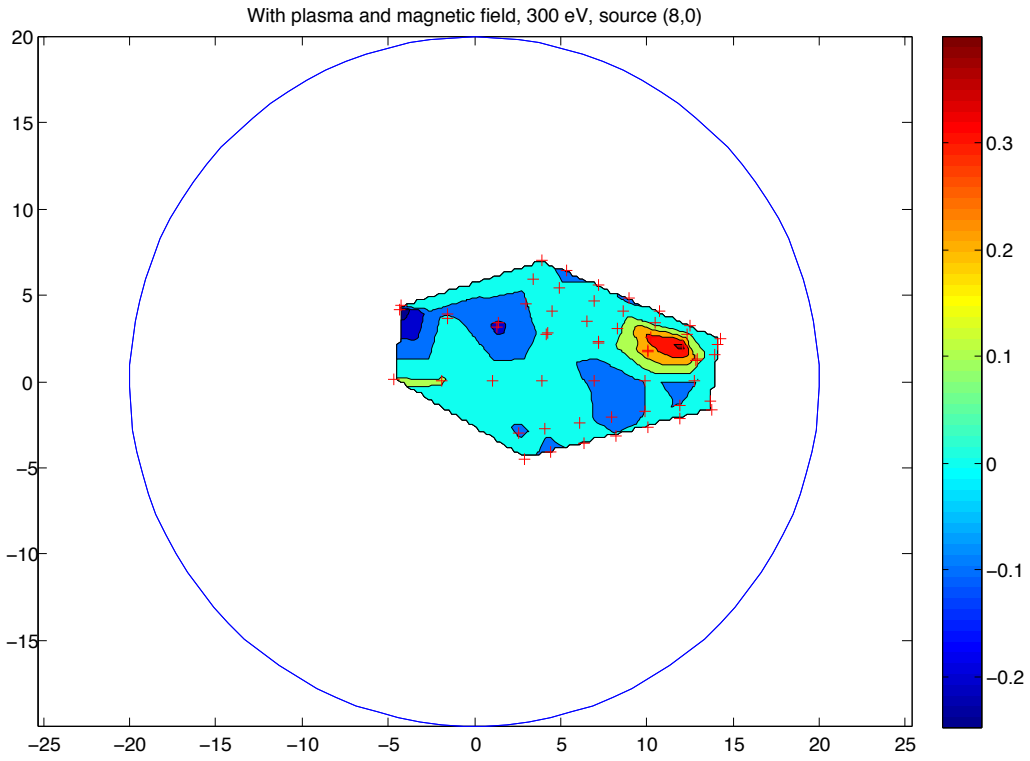

Figure 5.12: Ions' current on the detector, energy's ions of 300 eV.

We have made a zoom of the part of the profile where we see the ions' beam.

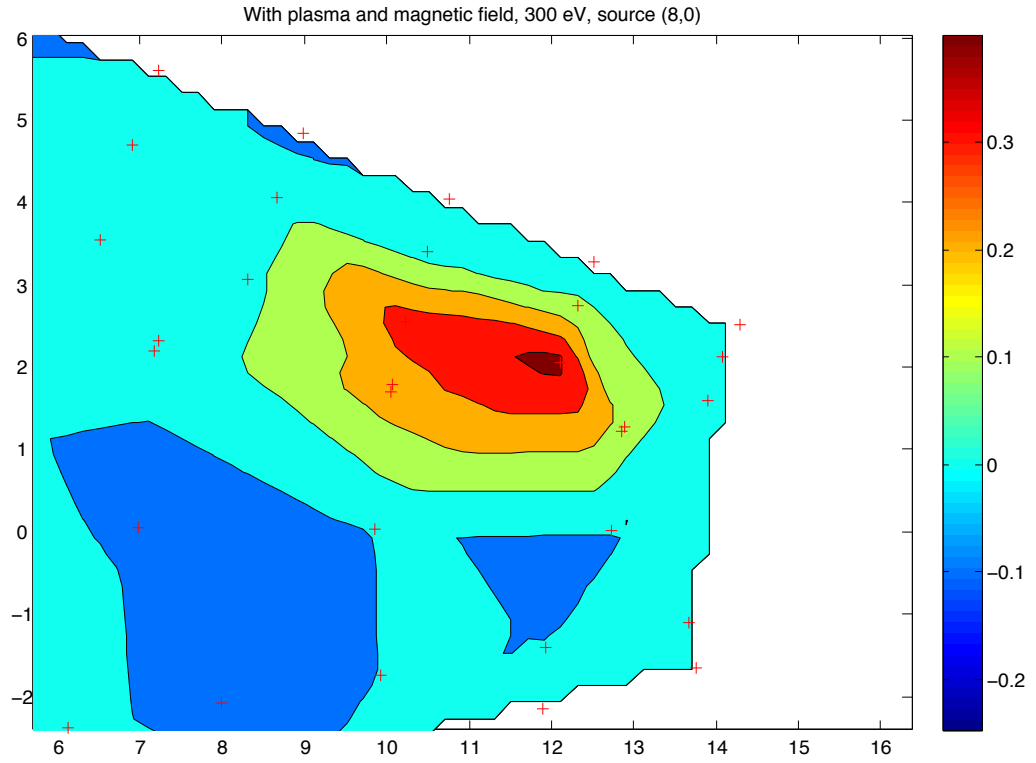

Figure 5.13: Zoom of the ions' current on the detector, energy's ions of 300 eV.

As we can see on the scale, a part of the graph has negatives value. We think that is due to peaks that appear when we move the system. These peaks are illustrated in chapter 6. The total current measured and calculated like in 5.1.1 is $0.1092\mu A$, on the source's external grid it was between 1.2 and 1.65 μA. We have on the followings graph vertical and horizontal cuts of the beam run through the maximum of the profile (measured at (12,2)).

The size of the beam is smaller than in the case without plasma and without magnetic field. The width at half height is about 3 cm on the horizontal axis and 1.6 cm on the vertical axis.

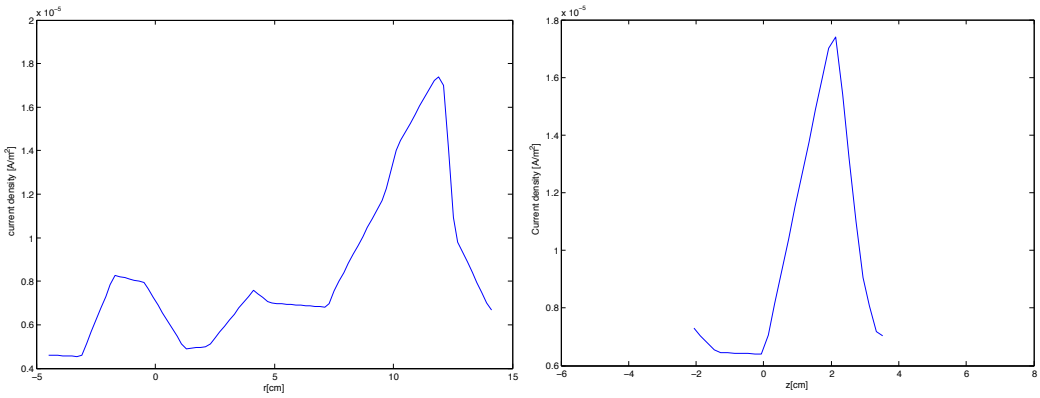

Figure 5.14: Horizontal and vertical cut of the ions' beam profile.

5.3.2 Profile With 500 eV

We have made the same measure for the ions' beam of 500 eV. We have on the two next figures the profiles measured.

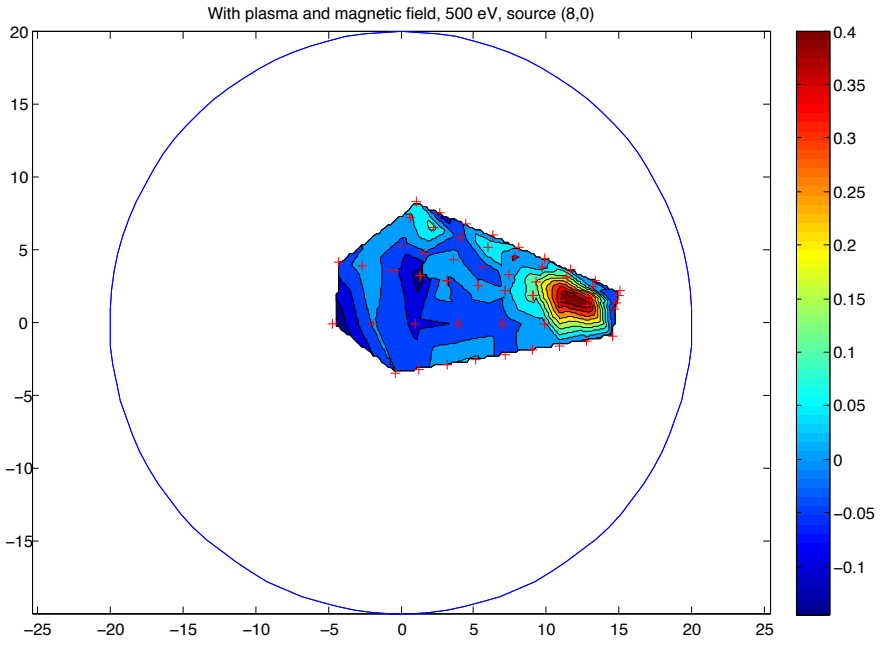

Figure 5.15: Ions' current on the detector, energy's ions of 500 eV.

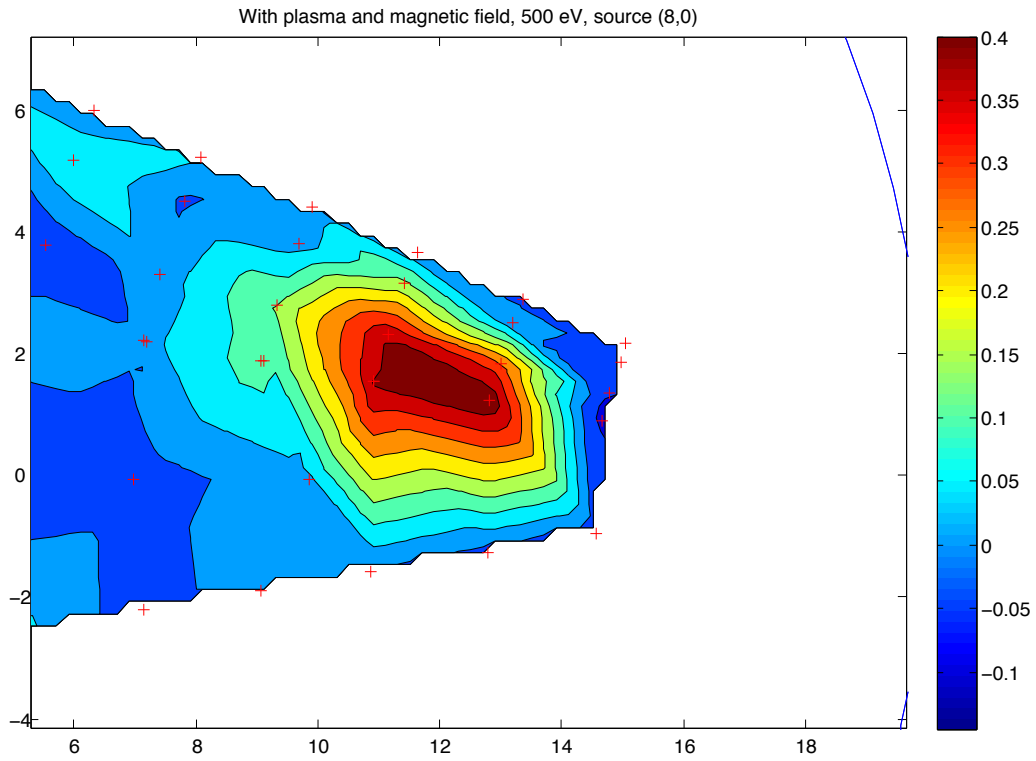

Figure 5.16: Zoom of the ions' current on the detector, energy's ions of 500 eV.

The current measured and calculated is $0.0653\mu A$ with between4.7 and 5.2 μA on the source's external grid. We have on the next figures the horizontal and vertical cuts of the beam (measured at (12.5,1.3)).

The width at half height is about 4 cm on the horizontal axis and 2.3 on the vertical one. An explantion can be the effect of the particles' energy on the Larmor radius (see eq 1.7). Particles with higer energy have higher Larmor radius.

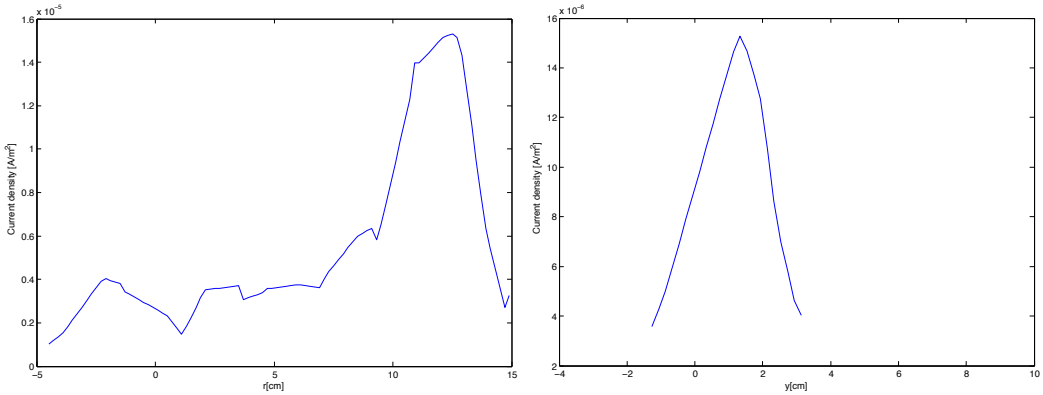

Figure 5.17: Horizontal and vertical cut of the ions'beam profile.

5.4 Post deadline measures

After the deadline to render this report, we tried to remake some profiles with a new emitter. We have on the following figure the profiles measured with this emitter with an energy of 300 eV and 500 eV. The source was at the position (8,0) and has a small tilt from the perpendicular direction, relatively to the poloidal plan of the source.

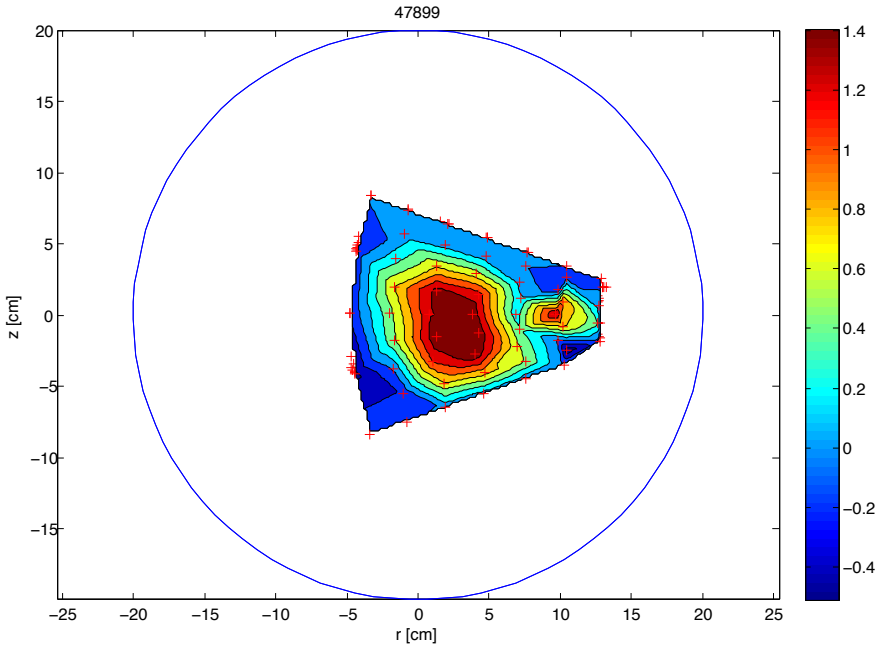

Figure 5.18: Ions' current on the detector, energy's ions of 300 eV.

We can see that there is something in the source that split the beam in two. It's possible that a small part of the isolation between the two grids in the source has been broken and make this split.

This time, the difference of current between the to profile is very smaller than the difference with the first emitter. The difference of current measured on the external grid of the source was very small too, this explain the difference.

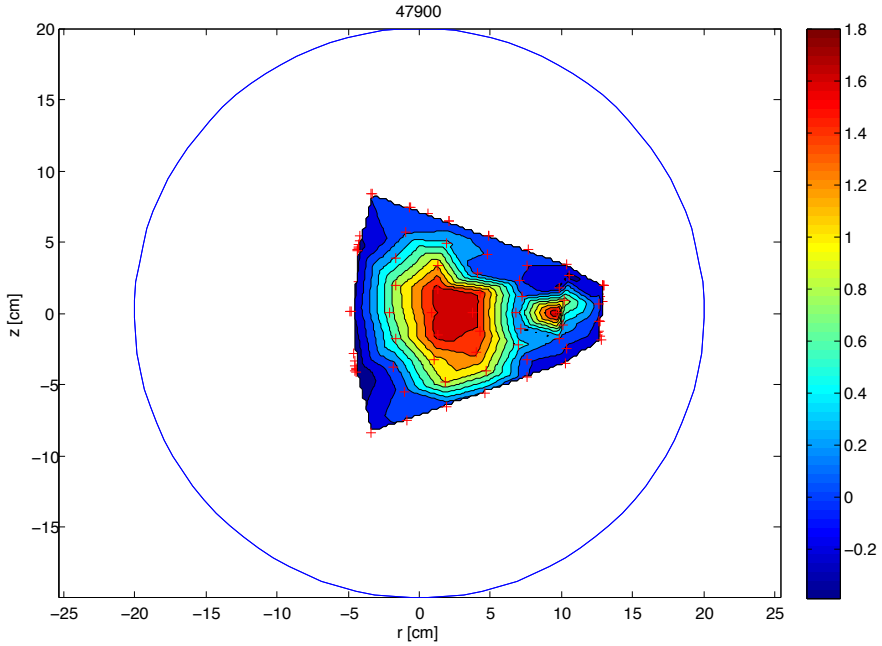

Figure 5.19: Ions' current on the detector, energy's ions of 500 eV.

Chapter 6

Discussion

The experimental results presented in chapter 5 raise some questions. What kind of ions' beam do we have with the 2^{nd} emitter? Is this beam isotropic? What is the energy distribution in the beam? Where does the effect seen with the magnetic field and with the 3^{rd} emitter come from? We try in this chapter to answer this question. In the first section, we will describe a simulation made to compare the results without magnetic field. In the second section, we discuss the capacitive effect which seems to influence the measures, by describing traces before and after the treatment with the lock-in device.

6.1 Comparison With Simulation

We have made some calibration simulation to know what the ions' beam looks like. These simulations are based on the code developed by Alice Burckel for her Master project in fall 2008 [8].

6.1.1 Description of the Code

Geometry

A natural coordinate system to describe the geometry of TORPEX is the cylindrical coordinate. The problem with this system comes from the magnetic field of TORPEX. As said in chapter 2, the magnetic field has two components, a toroidal magnetic field B_{th} and a vertical one. This means that the magnetic lines are tilted up by an angle $\theta = atan\frac{B_z}{B_{th}}$.

The two coordinate systems are linked through the standard equation system:

$$\hat{e_{\psi'}} = cos(\theta)\hat{e_{\psi}} + sin(\theta)\hat{e_z} \quad (6.1)$$

$$\hat{e_{z'}} = -sin(\theta)\hat{e_{\psi}} + cos(\theta)\hat{e_z} \quad (6.2)$$

In this system, we neglect the dependence in r of θ, $\theta = \theta(r = R)$.

Equations of Motion

Fast ions injected in the plasma interact with the magnetic field and the turbulent electric field created by the plasma itself [8]. If we neglect the collisions between fast ions and plasma particles or neutrals we have for the equations of motion:

$$\frac{d\vec{r}}{dt} = \vec{v} \quad (6.3)$$

$$m\frac{d\vec{v}}{dt} = q(\vec{E}(\vec{r},t) + \vec{v} \times \vec{B}(\vec{r},t)) \quad (6.4)$$

In our case, this system will be solve with $\vec{B} = \vec{E} = 0$.

Algorithm

To solve the equations of motion described before numerically, we need to discretize them and find an algorithm that gives for each step of the discretization the position $\vec{r}$ and the velocity $\vec{v}$ in function of the previous value $\vec{r}$ and $\vec{v}$. To solve this, Alice has chosen the Boris algorithm [9]. The equations of motion discretized with this algorithm become:

$$\frac{\vec{r}^{(n+1/2)} - \vec{r}^{n-1/2}}{\Delta t} = \vec{v}^n \quad (6.5)$$

$$\frac{\vec{v}^{(n+1)} - \vec{v}^n}{\Delta t} = \vec{E}(\vec{r}^{(n+1/2)}) + \frac{\vec{v}^{(n+1)} + \vec{v}^n}{2} \times \vec{B}(\vec{r}^{(n+1/2)}) \quad (6.6)$$

Parameter of the Source

To be closer to reality, the particles simulated with this code need some parameters. They depend on the geometry of the source and the source's

components. It's the energy distribution, the initial position of the source, its inclination angle and the angle between the toroidal field lines and the source. The energy distribution is supposed to be a gaussian, the different angles depend on the results of the measurement without magnetic field.

6.1.2 Calibrations Simulation

Now, based on the profiles presented in 5.1.2, we have set the geometric parameter. The inclination angle is suppose to be 0. We make this supposition because the maximum of the profile is at the vertical position 0. The angle between the toroidal field lines and the source is calculated using the maximum of the profile and the position of the source. We know that the source is at the position (8,0), the distance between the source and the detector's plan is 12.86^o and the position of the maximum is (4,0). The angle between the toroidal field lines and the source is 16.1^o.

Based on this data and knowing the total current measured by the detector, we have launched the simulation to find the the magnitude spreading, the injection shape and if it's isotropic. The conclusion of the simulation is a magnitude spreading of 1% and an isotropic shape cone with a spread of 4.73^o. The result is illustrated on the following graph.

The resolution of the graph is 0.6 cm in both direction. This choice is based on the size of the detector. The hole has a diameter of 0.6 cm.

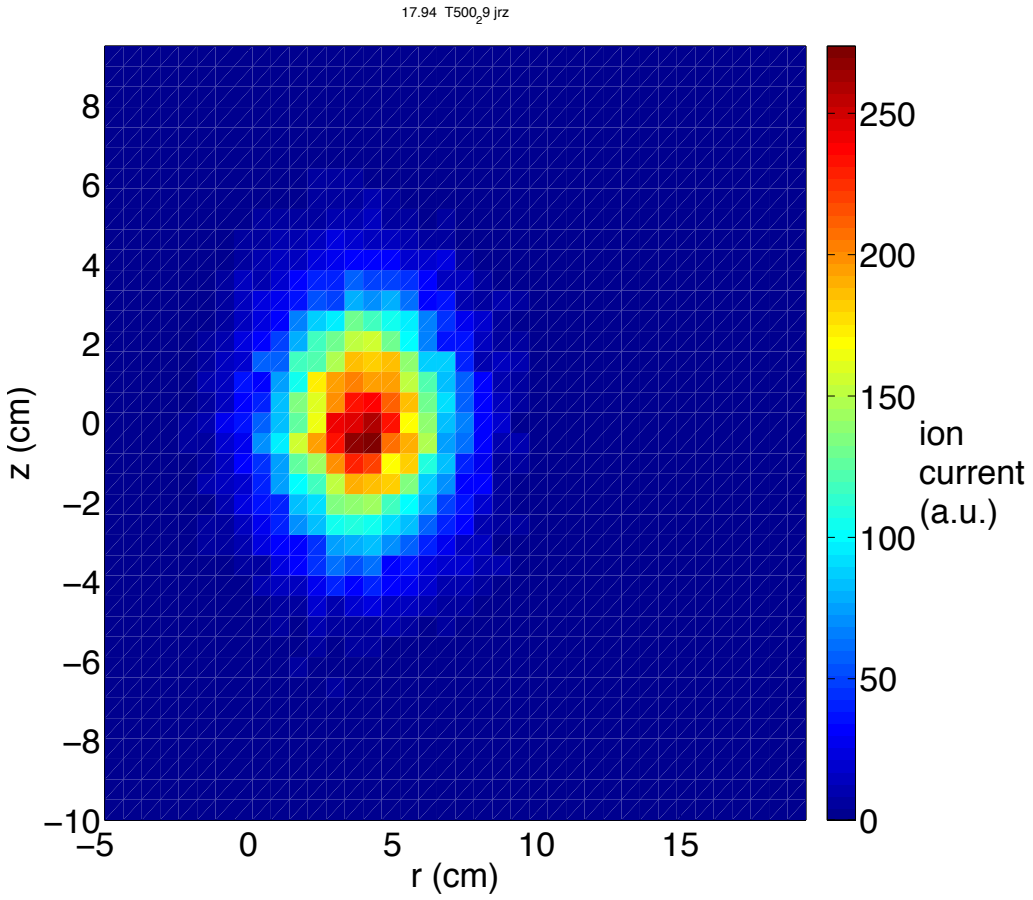

Figure 6.1: Result of the calibration simulation

These results looks quite similar to the profile of the figure 5.6. The position of the maximum is the same and the spreading in the horizontal and vertical direction are nearly the same.

6.2 Capacitive Effect

We will now discuss the problem raised by the figures 5.8, 5.9, 5.10 and 5.11. As said in chapter 5, we think that this problem comes from a capacitive effect. The current created by a capacitor is lead by the equation:

$$I = C\frac{dU}{dt} \tag{6.7}$$

I is the current created by this effect, C is the constant capacitance, U the bounded voltage and $\frac{dU}{dt}$ it's time variation. In our case, the bounded voltage is the ground for the detector and a voltage which depends on the time at the emitter. This voltage varies very fast during a small time and stays the same during the rest of the time. It's illustrated on the next figure.

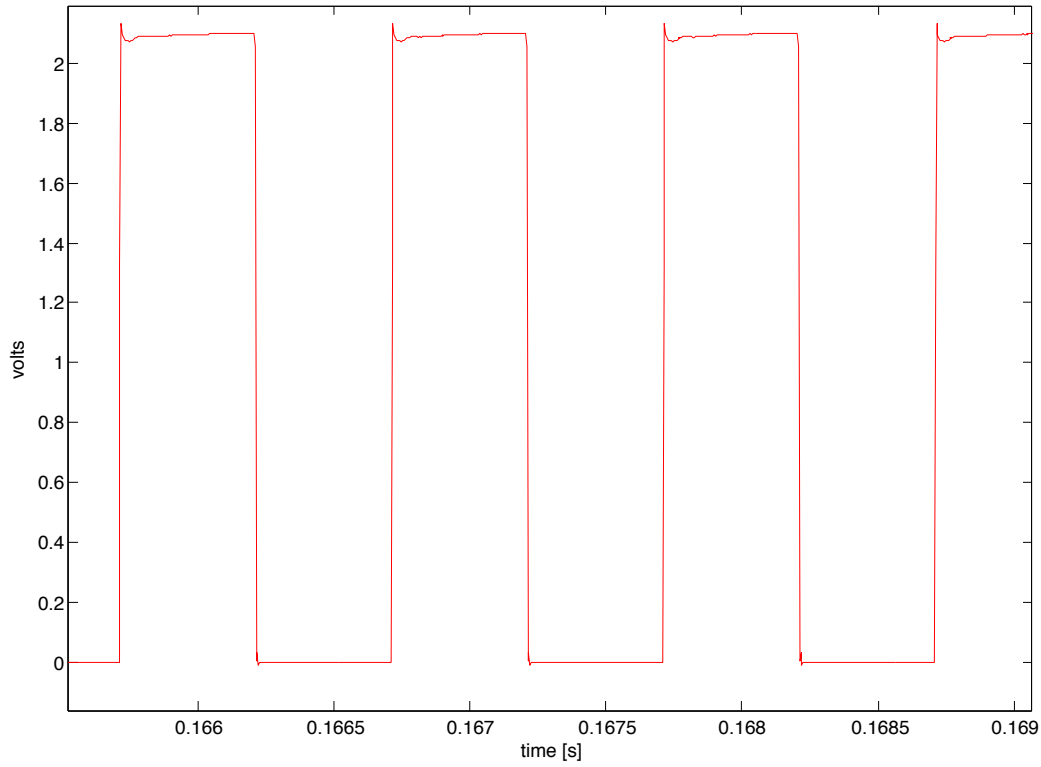

Figure 6.2: Polarisation apply on the emitter in function of the time.

On the next figure, we can see the translation of the probe (in voltage, a

high voltage means that the probe is introduced into the TORPEX) and the signal, measured just before the lock-in device. The horizontal axis is the time in seconds and the vertical one is the voltage measured. This measurement was done with the 3^{rd} emitter when it didn't seem to emit ions, without magnetic field. We can see two things on this graph, peaks appear when we move the detector and noise appear when the detector is introduced into the TORPEX.

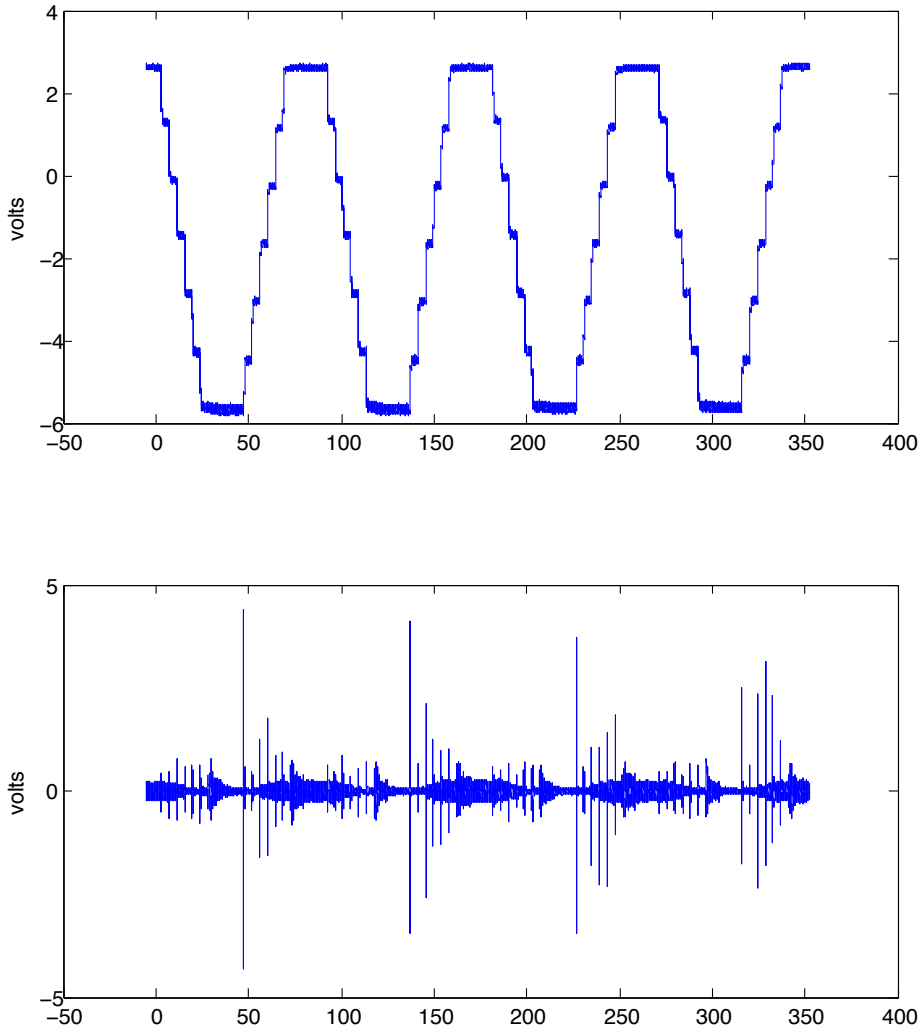

Figure 6.3: Trace measured before the lock-in device.

A zoom of this graph is presented on the following figure. This time the horizontal axis is the time in milliseconds. We can see the peaks created by the movement and the noise when the probe is introduced into TORPEX better.

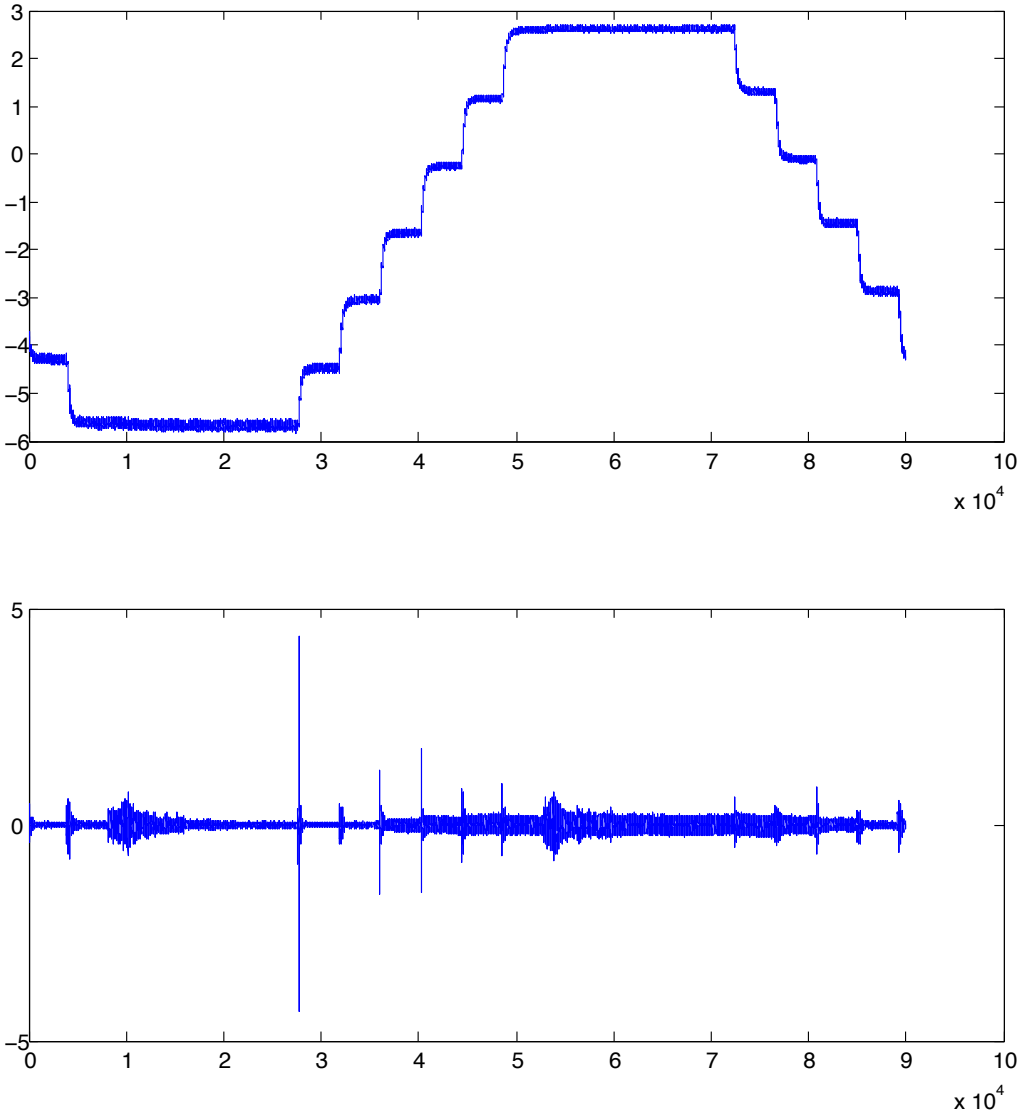

Figure 6.4: Zoom of the trace before the lock-in device.

To better understand the source of the effect observed on the figures 5.8,

5.9, 5.10 and 5.11, here are two interesting zooms, both from the previous trace. The first one, where the noise seems to be very small and the second where the noise is high.

On the second one, we can observe a signal which comes with a constant frequency. This frequency is the same as the frequency applied on the emitter, 70.9 Hz. Peaks are very thin and appear one time in positive, then in negative and then again in positive. We don't have the referential signal for the potential applied on the emitter, but it seems that the peaks correspond to a variation of the potential on the emitter.

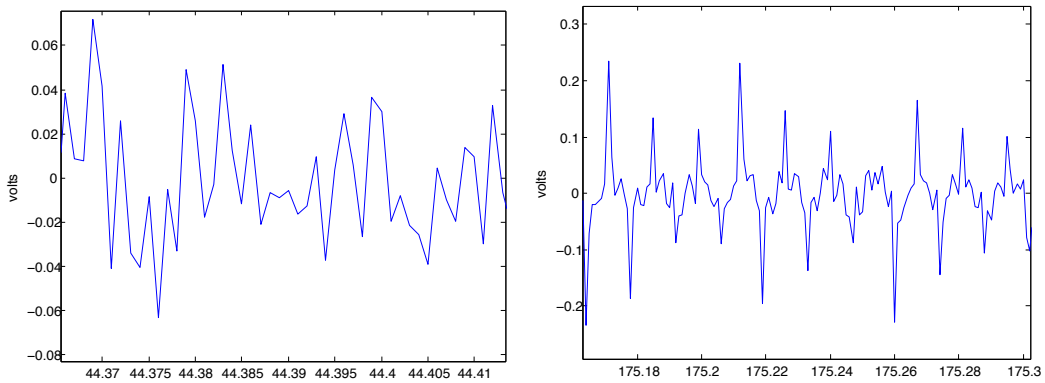

Figure 6.5: Zooms of the trace before the lock-in device.

6.2.1 Effect of the peaks

As we said before, peaks appear on the trace before the lock-in, when we move the probe, this peaks create other peaks after the lock-in. These effect is illustrated on the following figure. The axis are the time in horizontal, in milliseconds and the voltage measured out of the lock-in device. This trace was measured with an angle of 15^o for the detector.

We can see the points used to average the value measured in red, between these points we move the detector, it's at these moments that the peaks appear on the trace before the lock-in, and we can see peaks on this figure, after the lock-in too.

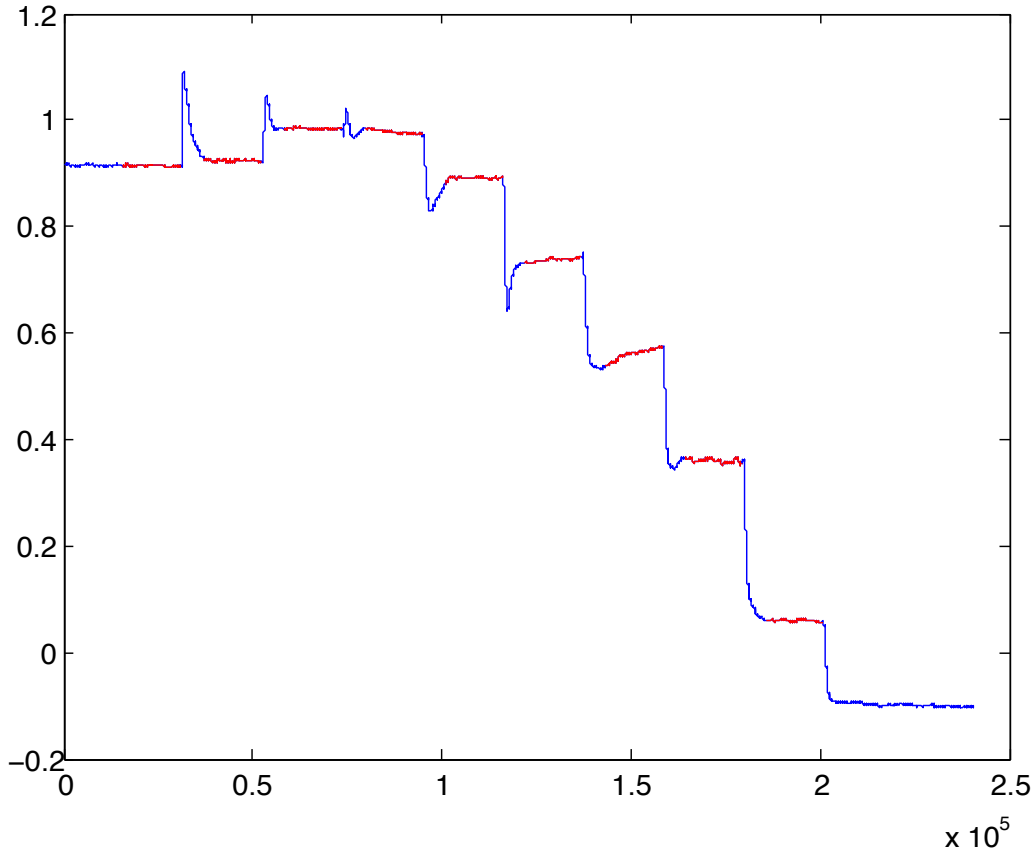

Figure 6.6: Trace measured after the lock-in device.

On the three following graphs, we can see zoom of this trace. the first one illustrated positive peaks, the two other negative peaks. On the second one, we can see that the value increases after a movement, it increase during the time we are averaging. This means that the peak created by the movement of the probe influences the value after the lock-in over a too long time.

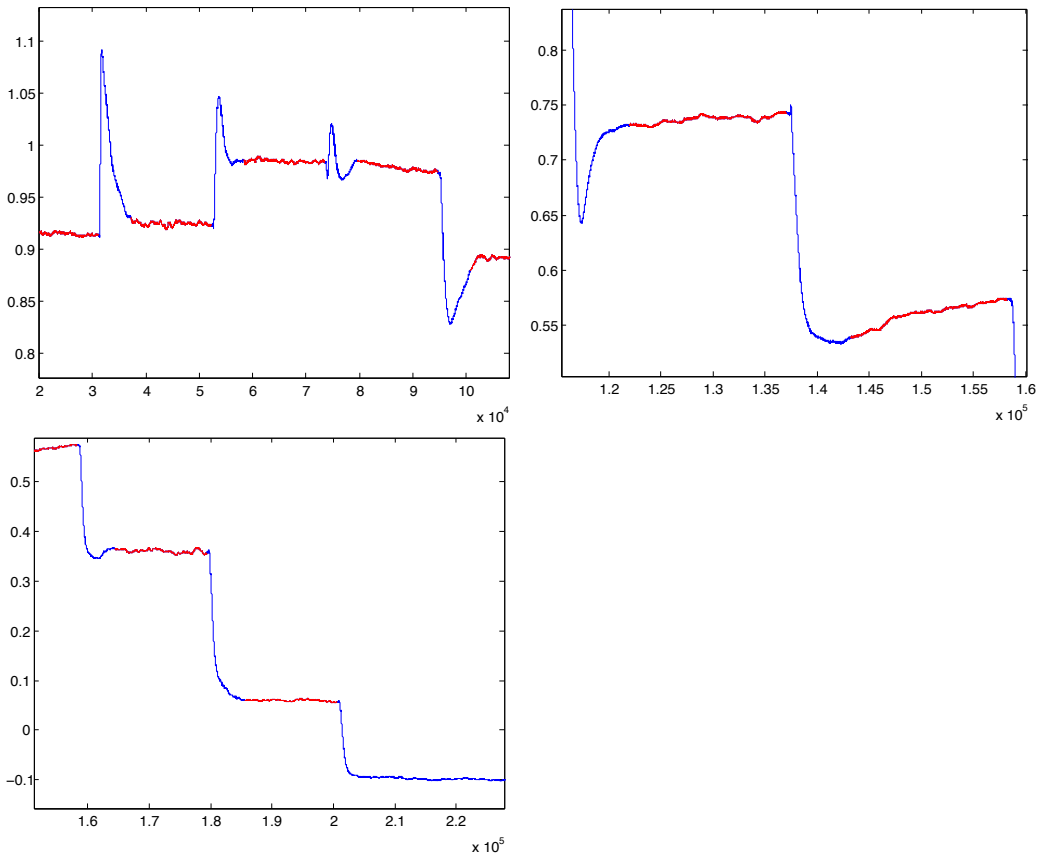

Figure 6.7: Zoom of the trace after the lock-in device.

It's hard to say if this effect influenced the measures with the plasma. On the next figures, we plotted two traces measured after the lock-in device, with plasma in the TORPEX, the axis are the same as without plasma. As we can see, the noise introduced by the plasma seems to be bigger than the peaks created by the movement of the probe.

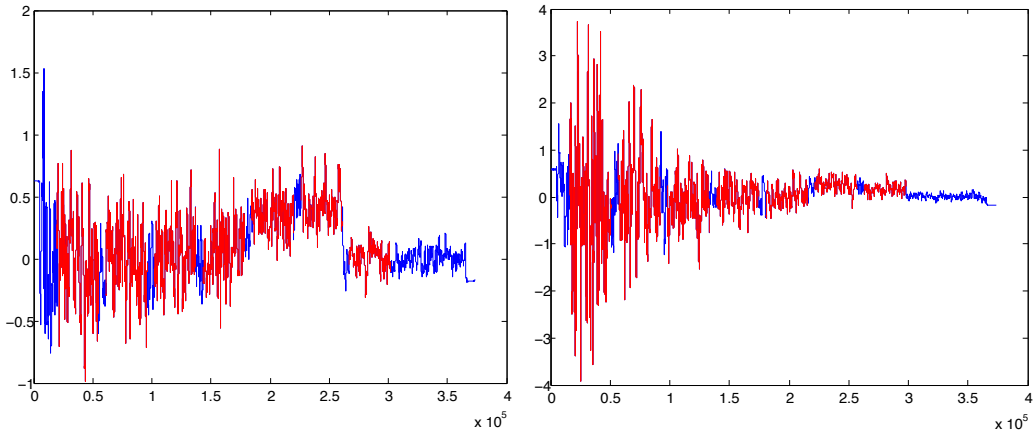

Figure 6.8: The trace after the lock-in device, with plasma.

These measure where made with an inclination of the detector of 15^o and 10^o degrees, the energy of ions is 300 eV, and the current measured on the external grid was between 1.54 and 1.65 μA. We can observe on the first one, that the average signal grows when it approaches the end of the measurement, then goes down, this corresponds to the maximum of the beam we can see on graph 5.12.

Chapter 7

Conclusion and Outlook

This diploma addressed basics question of how a fast ion beam interacts with the plasma, in changing the distance between the source and the detector and using different energies for the injected particles.

We first concentrated on the fast ion source. We tested different emitters and tried to understand why in certain cases an emitter mounted on the source can emit or not. The current of ions created by this source is very weak, about $1\mu A$. We then need to have a detector which can distinguish the fast ion from the background plasma noise. This was done using the setup developed for [1] and changing this setup to directly treat the data before the acquisition.

This new setup, called the lock-in, was used to measure fast ion profile. We made profiles without plasma and without magnetic field. We then added the magnetic field and finally the plasma. These experiments were conducted on the TORPEX machine.We have injected the ions in the blob region of the TORPEX.

These measurements demonstrate that we are able to make measurements at different points of the poloidal plane of TORPEX, in changing the position of the probe, during the same plasma shot. This method used with our setup can be used to make measurements with other probes equipped with motorized moving system. The measurements raised some problem of capacitive effect between the source and the probe. We need to take this effect into account, understand where it come from and how can we eliminate it, if

we want to go further in the investigation.

To go further in the investigation of fast ion dynamics in plasma, plans have been drawn for a movable system for the source. This system will provide movement of the source of the order of the millimeter. This system consist of the same source, mounted on a wagon. This wagon can move on a rail with an ultrasonic motor.

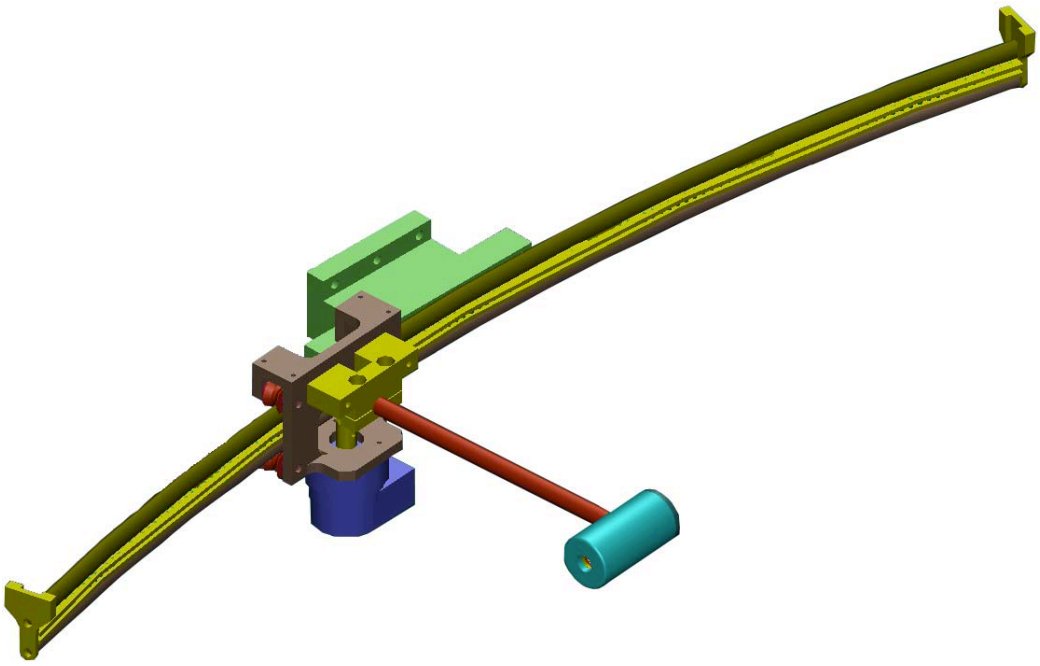

Figure 7.1: 3D illustration of the toroidal moving system of the source.

Ultrasonic motors use ultrasonic vibrations generated by piezo-electric ceramics as driving source. The ultrasonic motor will move only when a current traverses. When no current is presents, the motor blocks any movement. The motor use ultrasonic vibration to make contact between a part of the stator and the rotor, then it moves this part of the stator. An other part of the stator is then put in contact while the first stator is removed. The new contact can then move. The plan have been designed to use the USR30-E3a(E3N) from Shinsei Corporation [10].

The rail has been designed to be plugged into a movable sector from TORPEX. This imposes that it can't be longer than the sector but allows, for us, easier installation and maintainance. This rail will measure 59 cm long and stay horizontal, along the LFS border of the chamber, inside TORPEX.

As we can see on the illustration 7.1, the source will be attached to the wagon. This means that we won't we able to turn it, to introduced it into TORPEX or to change the inclination of the source. This also means, that we need a good a practical method to change the emitter. We need a system which reduces the risk of short circuits in the source and in the cable to the minimum.

Such device would provides a 3D resolution of fast ions' beam with a high resolution in the TORPEX.

Appendix A

Tests of the Emitters

We present here the details of the emitters' tests. Here are the tables of every tests. We have plotted; the time in min, the pressure in the chamber in mbar, the pressure at the entrance of the turbomolecular pump, the tension we apply at the border of the system, the current that goes trough it, the power of the current and the current measured on the collector. See chapter 3 for more details on this test.

Time [min]	P in the vessel	P at the pump	U [V]	I [A]	P [W]	I grid [μA]
0	4.20E-06	2.20E-07	0.5	0.3	0.15	0
30	5.70E-06	3.00E-07	1	0.6	0.6	0
60	8.70E-06	4.00E-07	1.5	0.8	1.2	0
90	6.90E-06	3.40E-07	2	1	2	0
120	7.20E-06	4.00E-07	2.5	1.2	3	0
150	8.30E-06	4.60E-07	3	1.3	3.9	0
180	9.20E-06	4.60E-07	3.5	1.4	4.9	0.005
210	9.40E-06	5.40E-07	4	1.5	6	0.011
240	1.00E-05	5.40E-07	4.5	1.7	7.65	0.03
270	1.20E-05	6.30E-07	5	1.7	8.5	0.044
300	1.40E-05	7.40E-07	5.5	1.8	9.9	0.061
330	1.50E-05	7.40E-07	6	1.9	11.4	0.083
360	1.70E-05	7.40E-07	6.5	2	13	0.104
390	1.80E-05	1.00E-06	7	2.1	14.7	0.114
420	2.10E-05	1.20E-06	7.5	2.1	15.75	0.113
450	2.50E-05	1.40E-06	8	2.2	17.6	0.114
480	2.10E-05	1.20E-06	8.5	2.3	19.55	0.091
510	3.30E-05	1.90E-06	9.9	2.5	24.75	0.082

Time [min]	P in the vessel	P at the pump	U [V]	I [A]	P [W]	I grid [μA]
0	1.40E-06	5.40E-08	0	0	0	0
10	1.60E-06	6.30E-08	0.5	0.3	0.15	0
20	2.30E-06	1.00E-07	1	0.6	0.6	0
30	2.20E-06	8.60E-08	1.5	0.7	1.05	0
40	2.10E-06	8.60E-08	2	0.8	1.6	0
50	2.20E-06	8.60E-08	2.5	1	2.5	0
60	2.20E-06	8.60E-08	3	1.1	3.3	0.001
70	2.30E-06	8.60E-08	3.5	1.2	4.2	0.002
80	2.40E-06	1.00E-07	4	1.3	5.2	0.019
90	2.70E-06	1.20E-07	4.5	1.4	6.3	0.042
100	3.20E-06	1.40E-07	5	1.5	7.5	0.067
110	3.50E-06	1.40E-07	5.5	1.6	8.8	0.107
120	3.80E-06	1.60E-07	6	1.7	10.2	0.147
130	3.90E-06	1.60E-07	6.5	1.8	11.7	0.17
140	4.30E-06	1.90E-07	7	1.9	13.3	0.154
150	4.80E-06	2.20E-07	7.5	2	15	0.145
160	5.40E-06	2.20E-07	8	2.1	16.8	0.139
170	6.00E-06	2.50E-07	8.5	2.2	18.7	0.123
180	6.70E-06	3.00E-07	9	2.2	19.8	0.106
190	8.00E-06	3.40E-07	9.5	2.3	21.85	0.077
200	9.60E-06	4.00E-07	10	2.4	24	0.054

Figure A.1: Details of 1^{st} and the 2^{nd} of the tests of the 1^{st} emitter.

Time [min]	P in the vessel	P at the pump	U [V]	I [A]	P [W]	I grid [μA]
0	1.80E-06	8.60E-08	0	0	0	0
30	3.10E-06	1.60E-07	0.5	0.4	0.2	0
60	2.50E-06	1.20E-07	1	0.7	0.7	0
90	2.40E-06	1.00E-07	1.5	0.9	1.35	0
120	2.50E-06	1.20E-07	2	1.1	2.2	0
150	2.60E-06	1.20E-07	2.5	1.2	3	0.001
180	2.90E-06	1.40E-07	3	1.3	3.9	0.011
210	3.20E-06	1.40E-07	3.5	1.4	4.9	0.02
240	3.70E-06	1.60E-07	4	1.6	6.4	0.077
270	4.10E-06	1.90E-07	4.5	1.7	7.65	0.291
300	4.50E-06	2.20E-07	5	1.7	8.5	0.413
330	5.30E-06	2.50E-07	5.5	1.8	9.9	0.599
360	6.30E-06	3.00E-07	6	1.9	11.4	0.387
390	6.80E-06	3.00E-07	6.5	2	13	0.275
420	9.70E-06	4.60E-07	7	2.1	14.7	0.615
450	1.30E-05	6.30E-07	7.5	2.2	16.5	0.645
480	1.80E-05	8.60E-07	8	2.3	18.4	0.633
510	2.20E-05	1.20E-06	8.5	2.4	20.4	0.82
540	2.50E-05	1.40E-06	9	2.4	21.6	1.212

Time [min]	P in the vessel	P at the pump	U [V]	I [A]	P [W]	I grid [μA]
0	1.70E-06	8.60E-08	0	0	0	0
10	1.80E-06	8.60E-08	0.5	0.6	0.3	0
20	1.80E-06	8.60E-08	1	0.8	0.8	0
30	1.90E-06	8.60E-08	1.5	1	1.5	0
40	1.90E-06	1.00E-07	2	1	2	0
50	1.90E-06	1.00E-07	2.5	1.1	2.75	0
60	2.00E-06	1.00E-07	3	1.3	3.9	0.006
70	2.10E-06	1.00E-07	3.5	1.4	4.9	0.016
80	2.20E-06	1.00E-07	4	1.5	6	0.05
90	2.30E-06	1.00E-07	4.5	1.6	7.2	0.095
100	2.50E-06	1.20E-07	5	1.7	8.5	0.141
110	3.00E-06	1.40E-07	5.5	1.8	9.9	0.117
120	3.00E-06	1.40E-07	6	1.9	11.4	0.107
130	3.60E-06	1.60E-07	6.5	2	13	0.091
140	4.30E-06	1.90E-07	7	2.1	14.7	0.158
150	5.80E-06	3.00E-07	7.5	2.2	16.5	0.219
160	6.90E-06	3.40E-07	8	2.2	17.6	0.326
170	8.00E-06	4.00E-07	8.5	2.3	19.55	0.58
180	1.20E-06	6.30E-07	9	2.4	21.6	0.967
190	1.70E-06	8.60E-07	9.5	2.5	23.75	1.735

Figure A.2: Details of 1^{st} and the 2^{nd} of the tests of the 2^{nd} emitter.

Time [min]	P in the vessel	P at the pump	U [V]	I [A]	P [W]	I grid [μA]
0	1.40E-06	7.40E-08	0	0	0	0
30	1.90E-06	8.60E-08	0.5	0.4	0.2	0
60	1.70E-06	8.60E-08	1	0.6	0.6	0
90	1.80E-06	8.60E-08	1.5	0.8	1.2	0
120	1.70E-06	8.60E-08	2	0.9	1.8	0
150	1.90E-06	8.60E-08	2.5	1.1	2.75	0.001
180	2.10E-06	1.00E-07	3	1.2	3.6	0.004
210	2.30E-06	1.00E-07	3.5	1.3	4.55	0.015
240	2.40E-06	1.00E-07	4	1.5	6	0.04
270	2.50E-06	1.20E-07	4.5	1.6	7.2	0.117
300	2.70E-06	1.20E-07	5	1.7	8.5	0.275
330	2.40E-06	1.00E-07	5.5	1.8	9.9	0.373
360	3.10E-06	1.40E-07	6	1.9	11.4	0.27
390	3.50E-06	1.60E-07	6.5	2	13	0.155
420	3.90E-06	1.90E-07	7	2.1	14.7	0.157
450	4.60E-06	2.20E-07	7.5	2.2	16.5	0.316
480	5.40E-06	2.50E-07	8	2.3	18.4	0.54
510	6.40E-06	3.00E-07	8.5	2.4	20.4	0.803
540	7.50E-06	3.40E-07	9	2.5	22.5	1.274

Time [min]	P in the vessel	P at the pump	U [V]	I [A]	P [W]	I grid [μA]
0	1.30E-06	5.40E-08	0	0	0	0
30	1.30E-06	5.40E-08	0.5	0.4	0.2	0
60	1.30E-06	6.30E-08	1	0.6	0.6	0
90	1.40E-06	6.30E-08	1.5	0.8	1.2	0
120	1.30E-06	6.30E-08	2	0.9	1.8	0
150	1.40E-06	6.30E-08	2.5	1.1	2.75	0.001
180	1.40E-06	6.30E-08	3	1.2	3.6	0.007
210	1.40E-06	6.30E-08	3.5	1.3	4.55	0.016
240	1.50E-06	6.30E-08	4	1.5	6	0.035
270	1.60E-06	7.40E-08	4.5	1.6	7.2	0.056
300	1.60E-06	7.40E-08	5	1.7	8.5	0.065
330	1.80E-06	8.60E-08	5.5	1.8	9.9	0.064
360	1.90E-06	8.60E-08	6	1.9	11.4	0.079
390	2.10E-06	8.60E-08	6.5	2	13	0.092
420	2.40E-06	1.00E-07	7	2.1	14.7	0.113
450	2.80E-06	1.20E-07	7.5	2.2	16.5	0.173
480	3.50E-06	1.60E-07	8	2.3	18.4	0.397
510	4.50E-06	2.20E-07	8.5	2.4	20.4	1.018
540	6.20E-06	3.00E-07	9	2.5	22.5	2.21

Figure A.3: Details of 1^{st} and the 2^{nd} of the tests of the 3^{rd} emitter.

Time [min]	P in the vessel	P at the pump	U [V]	I [A]	P [W]	I grid [μA]
0	1.20E-06	5.40E-08	0	0	0	0
30	1.70E-06	7.40E-08	0.5	0.3	0.15	0
60	1.50E-06	7.40E-08	1	0.6	0.6	0
90	1.60E-06	7.40E-08	1.5	0.8	1.2	0
120	1.60E-06	7.40E-08	2	0.9	1.8	0
150	1.70E-06	7.40E-08	2.5	1.1	2.75	0.001
180	1.90E-06	8.60E-08	3	1.2	3.6	0.003
210	2.00E-06	8.60E-08	3.5	1.4	4.9	0.019
240	2.40E-06	1.00E-07	4	1.5	6	0.043
270	2.20E-06	1.00E-07	4.5	1.6	7.2	0.075
300	2.50E-06	1.00E-07	5	1.7	8.5	0.135
330	2.80E-06	1.00E-07	5.5	1.8	9.9	0.133
360	3.00E-06	1.40E-07	6	1.9	11.4	0.141
390	3.30E-06	1.40E-07	6.5	2	13	0.086
420	3.70E-06	1.60E-07	7	2.1	14.7	0.081
450	4.20E-06	1.90E-07	7.5	2.1	15.75	0.148
480	4.60E-06	2.20E-07	8	2.2	17.6	0.299
510	5.30E-06	2.50E-07	8.5	2.3	19.55	0.634
540	6.20E-06	2.90E-07	9	2.4	21.6	1.083

Time [min]	P in the vessel	P at the pump	U [V]	I [A]	P [W]	I grid [μA]
0	1.20E-06	5.40E-08	0	0	0	0
10	1.20E-06	5.40E-08	0.5	0.4	0.2	0
20	1.30E-06	5.40E-08	1	0.6	0.6	0
30	1.30E-06	5.40E-08	1.5	0.8	1.2	0
40	1.30E-06	5.40E-08	2	0.9	1.8	0
50	1.30E-06	6.30E-08	2.5	1.1	2.75	0.001
60	1.30E-06	6.30E-08	3	1.2	3.6	0.004
70	1.40E-06	6.30E-08	3.5	1.3	4.55	0.013
80	1.40E-06	6.30E-08	4	1.5	6	0.022
90	1.50E-06	7.40E-08	4.5	1.5	6.75	0.034
100	1.60E-06	7.40E-08	5	1.6	8	0.049
110	1.70E-06	7.00E-08	5.5	1.7	9.35	0.062
120	1.80E-06	8.60E-08	6	1.8	10.8	0.053
130	2.00E-06	8.60E-08	6.5	1.9	12.35	0.034
140	2.20E-06	1.00E-07	7	2	14	0.069
150	2.50E-06	1.00E-07	7.5	2.1	15.75	0.146
160	2.90E-06	1.20E-07	8	2.2	17.6	0.347
170	3.60E-06	1.60E-07	8.5	2.3	19.55	0.619
180	4.50E-06	1.90E-07	9	2.4	21.6	1.16

Figure A.4: Details of 1^{st} and the 2^{nd} of the tests of the 4^{th} emitter.

On the following figures we have plotted the heating power in function of

Time [min]	P in the vessel	P at the pump	U [V]	I [A]	P [W]	I grid [μA]
0	1.90E-06	8.60E-08	0	0	0	0
30	2.20E-06	1.00E-07	0.5	0.3	0.15	0
60	2.80E-06	1.60E-07	1	0.5	0.5	0
90	3.00E-06	1.40E-07	1.5	0.8	1.2	0
120	2.80E-06	1.40E-07	2	1	2	0
150	2.80E-06	1.40E-07	2.5	1.1	2.75	0
180	3.10E-06	1.40E-07	3	1.2	3.6	0
210	3.40E-06	1.60E-07	3.5	1.3	4.55	0.001
240	3.50E-06	1.60E-07	4	1.5	6	0.003
270	3.30E-06	1.60E-07	4.5	1.5	6.75	0.006
300	3.60E-06	1.60E-07	5	1.6	8	0.001
330	4.00E-06	1.90E-07	5.5	1.7	9.35	0.003
360	4.80E-06	2.20E-07	6	1.8	10.8	0.007
390	5.50E-06	2.50E-07	6.5	1.9	12.35	0.019
420	6.30E-06	2.50E-07	7	2	14	0.044
450	7.30E-06	3.40E-07	7.5	2.1	15.75	0.083
480	8.90E-06	4.00E-07	8	2.2	17.6	0.135
510	1.10E-05	5.40E-07	8.5	2.3	19.55	0.199
540	1.50E-05	7.40E-07	9	2.4	21.6	0.29
570	1.80E-05	8.60E-07	9.5	2.5	23.75	0.335
600	1.80E-05	8.60E-07	10	2.6	26	0.37

Time [min]	P in the vessel	P at the pump	U [V]	I [A]	P [W]	I grid [μA]
0	1.60E-06	8.60E-08	0	0	0	0
10	1.70E-06	8.60E-08	0.5	0.5	0.25	0
20	1.70E-06	8.60E-08	1	0.7	0.7	0
30	1.70E-06	8.60E-08	1.5	1	1.5	0
40	1.80E-06	8.60E-08	2	1.1	2.2	0
50	1.80E-06	8.60E-08	2.5	1.2	3	0
60	1.80E-06	8.60E-08	3	1.3	3.9	0
70	1.90E-06	8.60E-08	3.5	1.3	4.55	0
80	2.00E-06	1.00E-07	4	1.4	5.6	0
90	2.10E-06	8.60E-08	4.5	1.5	6.75	0
100	2.20E-06	1.00E-07	5	1.6	8	0
110	2.40E-06	1.20E-07	5.5	1.7	9.35	0.002
120	2.70E-06	1.20E-07	6	1.8	10.8	0.007
130	3.00E-06	1.40E-07	6.5	1.9	12.35	0.022
140	3.60E-06	1.60E-07	7	2	14	0.054
150	4.10E-06	1.90E-07	7.5	2.1	15.75	0.089
160	4.30E-06	2.50E-07	8	2.2	17.6	0.138
170	6.40E-06	3.00E-07	8.5	2.3	19.55	0.171
180	8.30E-06	4.00E-07	9	2.4	21.6	0.259
190	1.10E-05	5.40E-07	9.5	2.5	23.75	0.325
200	1.60E-05	7.40E-07	10	2.6	26	0.368

Figure A.5: Details of 1^{st} and the 2^{nd} of the tests of the emitter reloaded in Hungary.

the time, the current on the collector in function of the time and the current on the collector in function of the heating power.

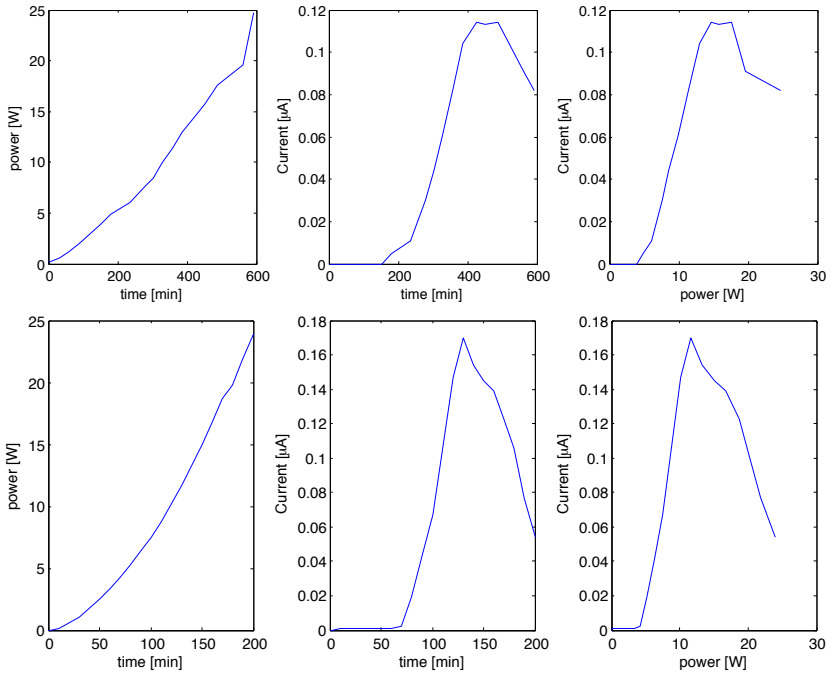

Figure A.6: Graphs of 1^{st} and the 2^{nd} of the tests of the 1^{st}emitter.

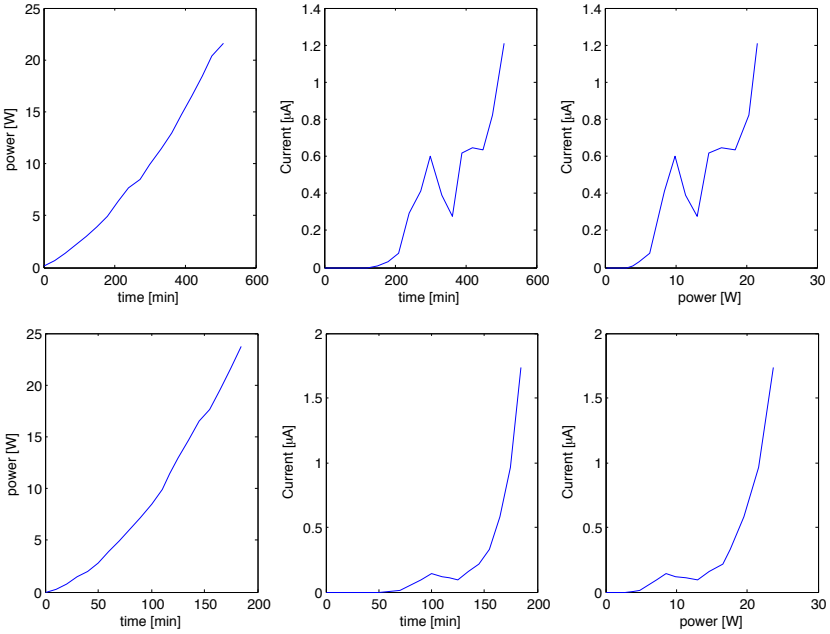

Figure A.7: Graphs of 1^{st} and the 2^{nd} of the tests of the 2^{nd}emitter.

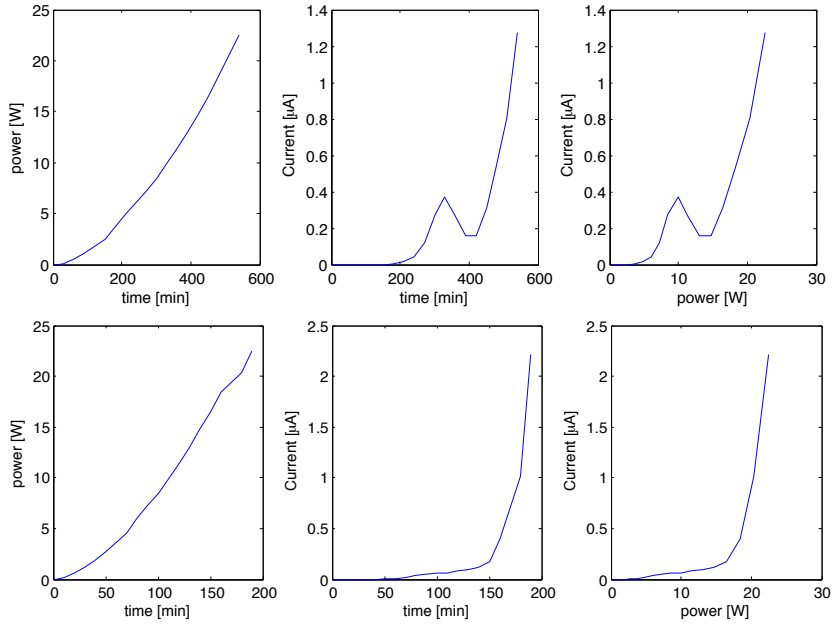

Figure A.8: Graphs of 1^{st} and the 2^{nd} of the tests of the 3^{rd}emitter.

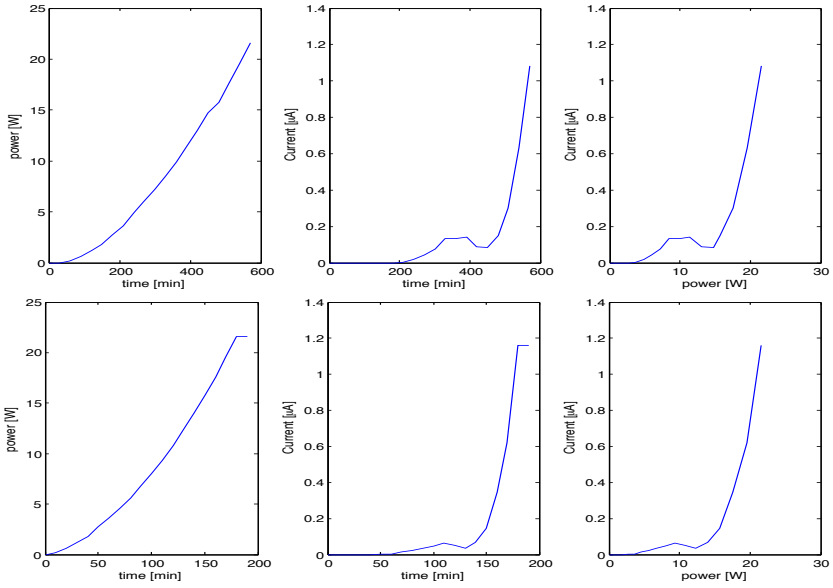

Figure A.9: Graphs of 1^{st} and the 2^{nd} of the tests of the 4^{th}emitter.

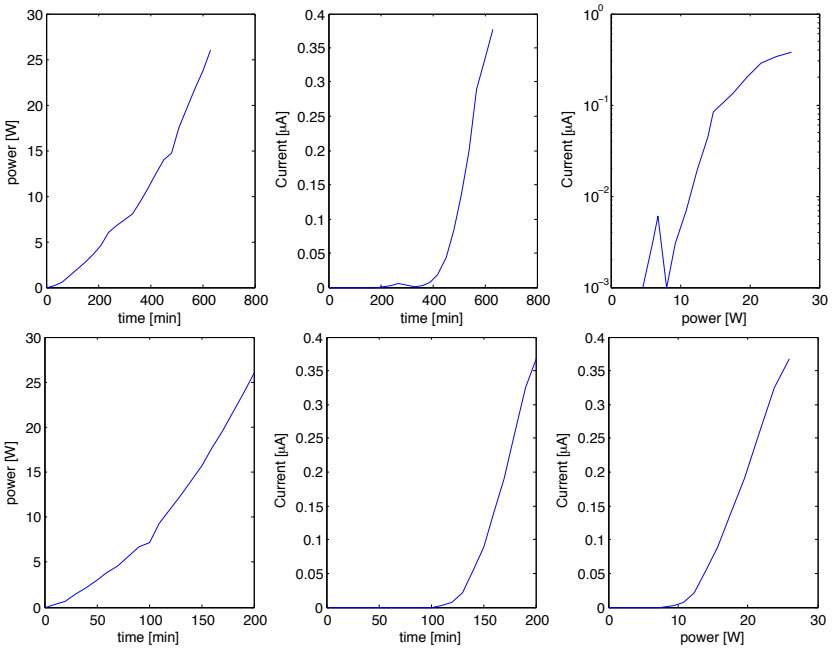

Figure A.10: Graphs of 1^{st} and the 2^{nd} of the tests of the emitter reloaded in Hungary.

Appendix B

Plan of the Source's Toroidal Moving System

Here is the plan drawn for the source's toroidal moving system, presented in chapter 7. This plan has been drawn to be printed in a A0 paper.

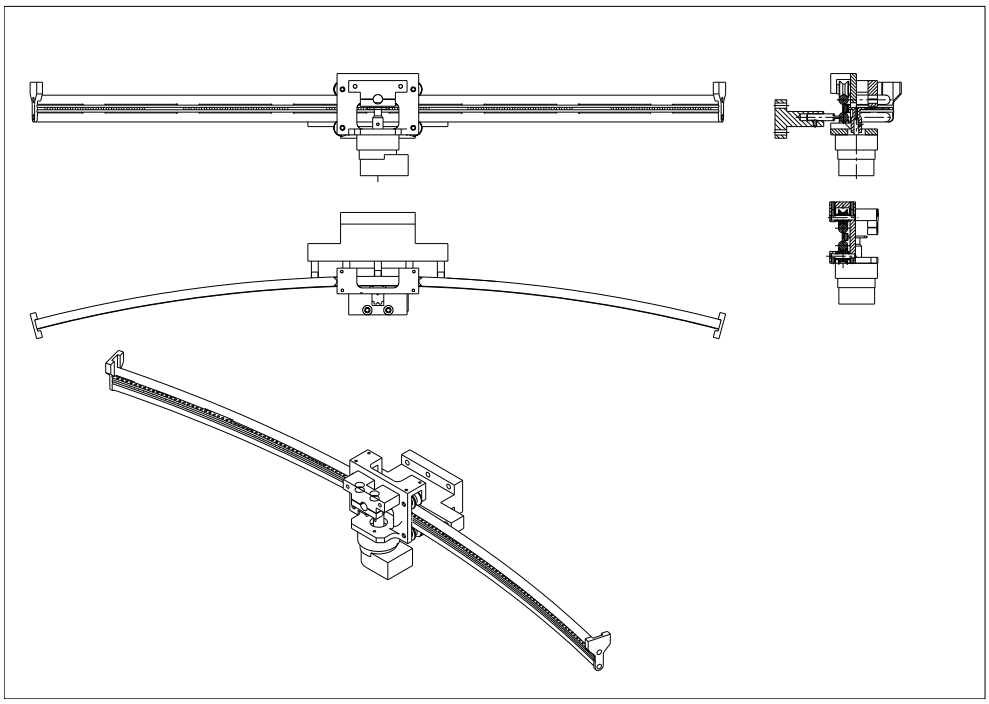

Figure B.1: Plan of the source moving system.

Appendix C

Mode d'emploi montage de la source

Nous décrivons ici le montage d'un émetteur sur la source. Cette opération doit être faites soigneusement et en faisant attention à un grand nombre de détails. En effet, une partie des montages ne fonctionnant pas était dut à des erreurs survenu lors du montage.

C.1 Piece à disposition

Pour monter un émetteur sur la source il faut:

- Support de la source
- Couvercle du support
- 4 pieces de support de grille
- 6 vis et 6 écrous pour les supports de grille
- Grillage en tungstène (w 50 my d 0.028 mm (325 mesh))
- 2 pièce de support d'émetteur
- 3 vis et 3 écrous pour le support d'émetteur
- Anneau d'isolation

- Un tube en céramique (environ 7.9 mm de diamètre externe, 4.8 mm de diamètre interne et 41 cm de long)
- 3 tube en céramique (environ 2 mm de diamètre externe, 1.5 mm de diamètre interne et 41 cm de long)
- Fils pour bobine en duramit, 0.6 mm et 0.3 mm de diamètre (prendre des bout bien assez long)
- Système de support pour la source avec tube en inox
- gaine thermorétractable
- Petit tube en céramique de très petit diamètre
- Cosse à sertir de différent diamètre

C.2 Préparation des grilles

La première chose a faire avant de monter la sonde et de préparer les différentes pièces, en commençant par les grilles.

Commencez par couper 2 morceaux de grillages. Ils doivent être plus gros que les trous des supports à grilles mais plus petits que les support eux même. La figure suivante illustre ce concept.

Une fois les morceaux de grille coupé, il faut les fixer entre les supports. Pour ce faire, la meilleur manière trouver pour le moment et de préparer les écrous, en vissant des deux partie du support sans rien entre 2. De cette façon il est possible de placer directement l'écrou au fond du trou prévu pour lui. Il sera plus facile après (une fois la grille et le fil de contacte entre les supports et que les vis auront juste la bonne taille) de visser les pièces ensemble. Il est possible d'utiliser des vis plus longues pour faciliter cette étape. Une fois les écrous en place, dévisser le tout sans sortir les écrous, placer la grille entre les deux support en faisant bien attention à laisser libre le chemin que les vis vont emprunter, soit en coupant la grille soit en la perçant, puis visser le tout. Une fois ceci en place, vérifier que la grille et aussi plate que possible et qu'elle cache bien tout le trouve des support.

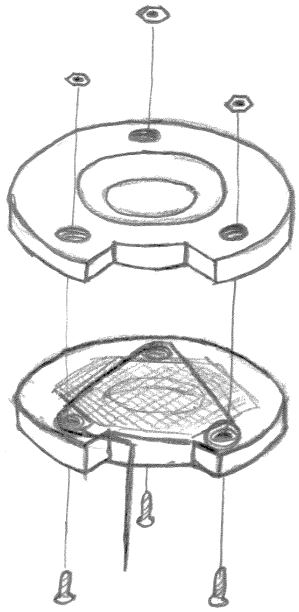

Figure C.1: Installation de la grille.

Il ne reste maintenant plus qu'à placer le fil dans le support. Pour ceci, choisir le fil de 0.3 mm de diamètre et en couper un bout bien assez long, 1.5 m est un minimum mais mieux vaut être généreux ça évite des problème par la suite. Dénuder un bout du fil sur minimum 6 cm (un fois encore, mieux vaut se montrer généreux et ne pas laisser de gaine). Le fil va devoir assurer la connexion entre la grille et l'extérieur, il faut donc s'assurer que le contacte et bien fait. Pour ceci, le fil fera 2/3 de tour du trou des support, entre les deux support en contournant les vis (voir figure précédante). La technique la plus pratique utilisé et d'écarter légèrement les deux supports en les dévissant un petit peut (sans sortir les écrous), une fois ceci fait, en faisant un léger crochet avec le bout du fil, l'amarrer à une vis, faire le tour des deux autre puis sortir. Il faut commencer par une vis a coté l'encoche des support, partir vers celle le plus loin de l'encoche et revenir vers la dernière de sorte que le fil va sortir directement par l'encoche. points A, B et C de la figure suivante. figure suivante.

Une fois cette opération terminer pour les deux grilles, il faut mettre sur chaqu'un des fils un petit tube en céramique qui servira de gaine à l'intérieur,

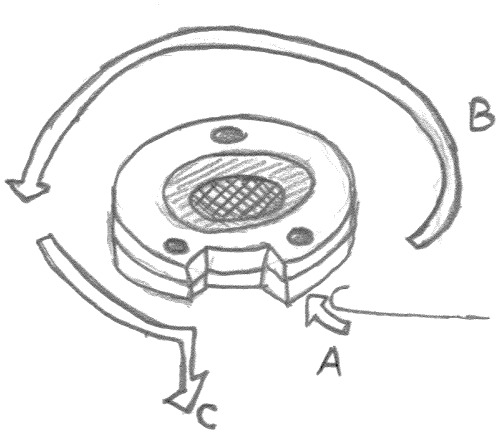

Figure C.2: Installation du fil sur la grille.

un d'environ 22 mm de long et un autre d'environ 17 mm. Le plus long sur le fil de la grille externe (un des supports fait un angle droit des deux côtés du trou).

C.3 Préparation de l'émetteur

Il faut maintenant prépare l'émetteur en le montant sur son support. Le support est constitué de deux pièces. Une avec un gros trou et une avec deux petit trous. Le gros trou est la pour accueillir le gros cylindre de l'émetteur, les petits trous sont là pour les filament de chauffage. Les deux pièces seront visées entre elle, il faut donc une nouvelle fois préparer les écrous de la même manière que pour les support des grilles. Les vis vont dans la pièce avec les 2 petits trous et les écrous dans l'autre.

Il faut avant de placer l'émetteur dans le support, tordre les 3 broches se trouvant sur les cotés du cylindre de l'émetteur, à 90^o par rapport au bord du cylindre, puis placer les filaments de chauffage dans les trous du support, en tournant l'émetteur de sort qu'une des broche sorte au niveau de l'encoche du support (voir figure suivante)

La broche qui sort au niveau de l'encoche sera utilisé pour mettre la cylindre de l'émetteur à un potentiel positif, les autres doivent être coupés si ils

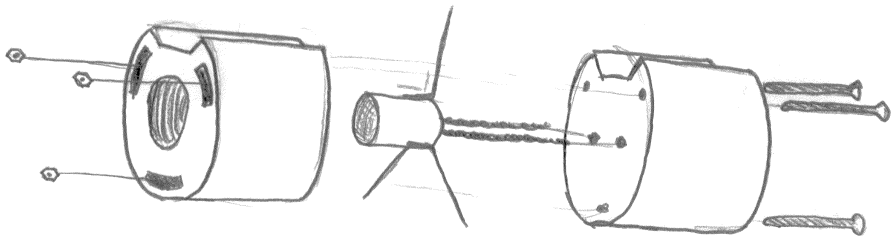

Figure C.3: Position de l'émetteur sur les supports.

dépassent du support. On place ensuite la deuxième pièce de support. Il faut viser les deux pièces entre elles. Lors que ces visé, il faut que les deux supports soit bien parallèles et que le cylindre de l'émetteur ne touche pas les bords intérieurs du support.
Il faut maintenant préparer le relai pour mettre au potentiel positif le cylindre de l'émetteur. Pour cela on prend un bout de fil de duramit de 0.6 mm de diamètre et quelque centimètre de long (prendre trop permet de couper après). Le fil doit être entièrement dénudé. La broche sortant des supports et de nouveau tordu à 90^o en direction des filaments de chauffage. On sertit ensuite avec une cosse à sertir la broche avec le fil que l'ont vient de dénudé. Il faut ensuite tordre le fil de sorte qu'il suive le support jusqu'à un des filaments de chauffage (voir figure suivante) il est préférable que ce fil arrive sur l'extérieur par rapport au filament.

Reste maintenant à préparer les deux fils pour alimenter l'émetteur. Prendre 2 fils duramit de 0.6 mm de diamètre et comme pour les grilles les prendre bien assez long et en dénuder un des bout sur quelques centimètre.

C.4 Assemblage de la source

On peut maintenant placer les différent élément dans la source. On met d'abord les pièces qui se trouveront vers la sortie des ions. La grille externe, un anneau d'isolation, la grille interne, un autre anneau d'isolation puis le support de l'émetteur avec les filament de chauffage vers l'arrière (voir figure

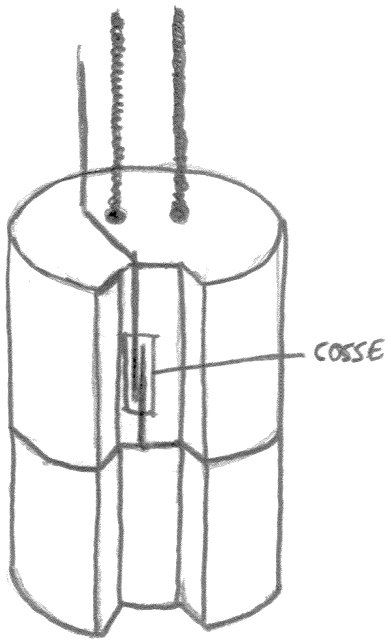

Figure C.4: Emetteur dans les supports.

suivant).

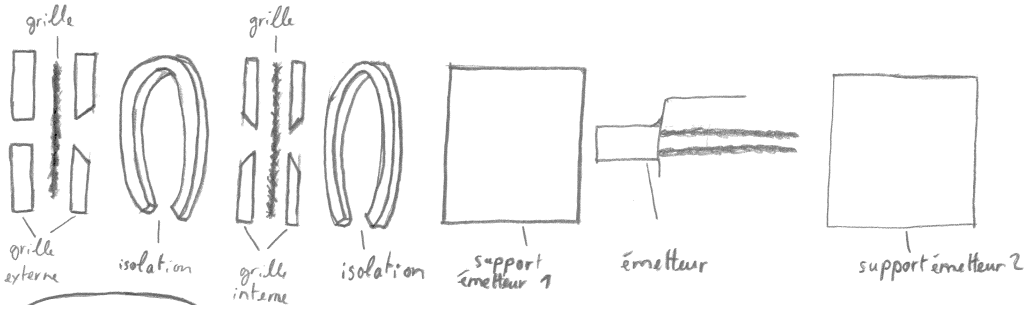

Figure C.5: Installation du fil sur la grille.

Cette opération est délicate, il faut faire attention à de nombreux points. Le support de l'émetteur est un cylindre creux avec un petit trou à une des extrémités (qui sera nommé l'avant de la source), un trou sur un des cotés, plus en arrière. Le support est ouvert à l'arrière avec un pat de vis pour le couvercle.

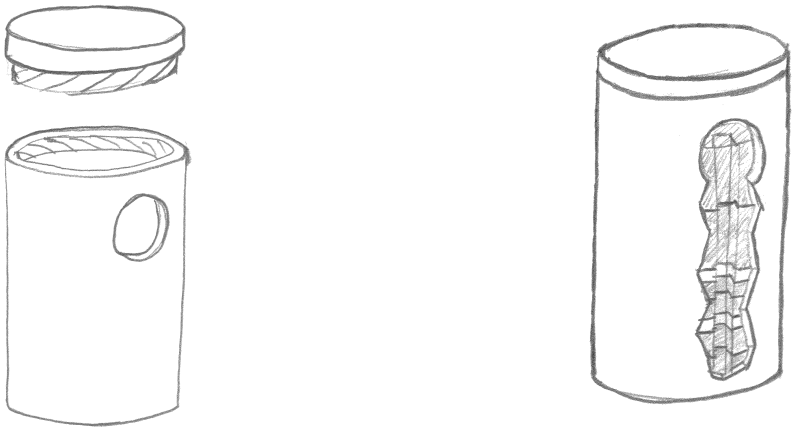

Figure C.6: Support de la source et support de la source "éclaté" sur le coté

Il faut placer chaque pièce séparément. Une fois chaque support de grille en place, faire passer le fil par le trou latéral du support et tourner le support de sorte que l'encoche soir du coté du trou. Faire de même pour les anneaux pour laisser passer les fils des grilles. Lors qu'on sort les fils des grilles par le trou, il faut pas que le fil fasse un angle ou un noeud, ça le fragiliserait. Utilisez plusieurs outils et faites de grand tour de l'intérieur de la source pour éviter cela. On peut aussi tourner le support de la grille pendant cette étape. Une fois les deux supports et les anneaux d'isolation en place, on peut placer le support de l'émetteur en plaçant de nouveau l'encoche du côté du trou latéral. Toute ces pièces, si elles sont bien en place, devraient arriver à mi hauteur du trou du support. On place ensuite les fils de 0.6 mm préparé en C.3 et on les sertit avec les filaments de chauffage sans oublie de mettre dans une des cosse un fil et un filament et dans l'autre cosse à sertir un fil, l'autre filament et le fil qui est relié à la broche de l'émetteur. Il faut maintenant couper les filament de chauffage de sorte qu'elle n'empêche pas de fermer le support de la source. Il est possible maintenant de placer des petits tube en céramique entre les différents fils afin de minimiser le risque de court circuit. On peut ensuite mettre un petit bout de tube en céramique autour d'un des filaments. Il servira a bien pousser le tour lorsqu'on ferme la source (on le fait maintenant). Il ne faut pas trop forcer en fermant la source, cela risque de casser un des anneaux d'isolation.

C.5 Assemblage au système de support

On fait maintenant passer les deux fils des grilles et un des fils de chauffage dans les 3 tubes en céramique de 2 mm de diamètre. On met ensuite ces 3 tubes et le dernier fil de chauffage dans le gros tube en céramique. Il faut bien choisir la position de chaque tube pour éviter tout croisement avant les tubes en céramique. Bien faire attention à la position du fil de chauffage, il ne peut croiser dans le gros tube en céramique.

Pour éviter tout oublie par la suite, mettre maintenant le gros anneaux blanc du système de support de la source avec tube en inox autour du tube en céramique. On place maintenant la gaine thérmorétractable autour des fils. L'idéal est bien sure de savoir qu'elle fil correspond à quelle grille et de leur attribuer un couleur. Pour les filaments de chauffage, cela à moins d'importance puisqu'ils n'ont pas le même diamètre et que le sens du courant de chauffage n'importe pas. Pour mettre facilement la gaine on peut la coupé en petits bouts. Si on choisit de la mettre par grand bout il faut la trouer avant afin de facilité le pompage. Une fois la gaine en place, on la rétracte à l'aide d'un foehn. On passe ensuite les fils dans le tube en inox du système de support. Place et vis le tube en céramique au tube en inox puis l'anneaux blanc. On doit maintenant coller le support de la source au tube en céramique. Le support doit être à 90^o par rapport au tube en inox. Il n'est pas facile d'avoir un bon angle. Si on place le tube à l'horizontale on peut caler le support avec des briques (si vous trouvez une meilleur manière de maintenir la source à 90^o par rapport au tube à un autre moment, il est possible de collé à ce moment là. Pour coller on utiliser la colle céramique "Hi-Purity Alumina Ceramic, Resbond 989" de COTRONIC corporation. Il faut bien remuer cette colle avant de l'appliquer. Une fois la colle en place, laissez sécher 4 heures minimum avant de remettre un autre couche si nécessaire ou de passer à la suite.

Reste maintenant à souder les connecteurs aux 4 fils sortant du système de support. Pour qu'il n'y aille pas de fils qui flotte, on dévisse le tube en céramique, on l'enfonce le tube en céramique dans celui en inox et on coupe les fils juste à la bonne longueur (mesuré avant d'enfoncé le tube en céramique). Ne pas oublier de dénuder 2 fois les fils (la gaine thérmorétractable et la gaine "naturel" des fils. Une fois les connections soudées, on remet le tube en place en fixant le connecteur (attention au joint) et on revisse le tube en

céramique.

C.6 Conclusion

Voilà, si tout à été bien fait, la source à été monté et est prête à être testé. Il faut savoir que ce mode d'emploie à été écrit selon les expérience de l'auteur, il peut donc y avoir des erreurs ou des améliorations possible. Il est arrivé que des courts circuits se sont formé lors de tests de la source après montage. une fois entre les fils et le système de support, d'ou la présence obligatoire des gaine thérmorétractable. Un court circuit est arrivé une fois entre la grille externe et la grille interne après chauffage (pas présent à l'origine) ce qui à conduit à l'apparition d'un courant négatif mesuré sur la grille externe. Il n'y pas été possible de comprendre la provenance ni la localisation de ce court circuit.

Appendix D

Câblage

Nous présentons ici les schéma de câblage utilisé avec notre matériel. Ceci est destiné, comme dans l'annexe C, à permettre de réutiliser le même matériel le plus facilement possible.

D.1 Boitier du détecteur

Le boitier du détecteur (voir photo D.1) se trouve à l'extérieur de TOPREX, il est relié par 6 câbles au détecteur, à l'alimentation du détecteur et à un amplificateur.

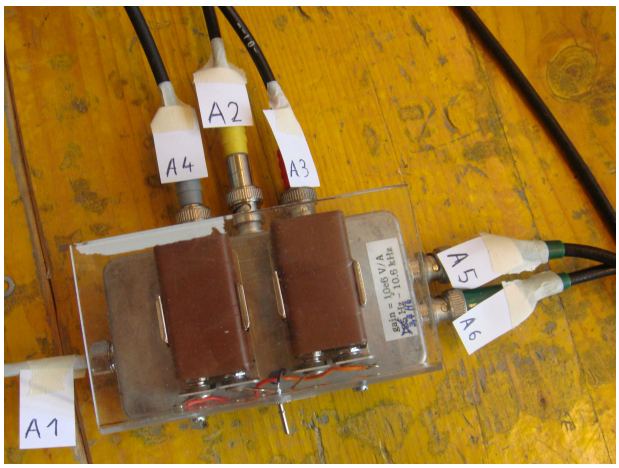

Figure D.1: Boitier du détecteur.

Le câble A1 relie le boitier au détecteur, les câbles A2, A3 et A4 à l'alimentation du détecteur et les câbles A5 et A6 à l'amplificateur, voir photo suivante.

Figure D.2: Câblage du boitier du détecteur sur: Le détecteur, l'alimentation du détecteur et l'amplificateur.

D.2 Lock-in

Une fois le signal amplifié il va par le câble B1 (photo D.2) vers le lock-in (photo D.3) le câble C1, branché avec un T à l'amplificateur et au câble B1, est branché soit à un oscilloscope, soit à l'acquisition soit aux deux.

Figure D.3: Lock-in.

Le cable B1 est branché au lock-in sur l'entrée SIGNAL IN, sur l'entré REF TTL on branche le câble B2 provenant de l'alimentation de la source (voir photo D.4). Tout comme le câble B1 sur l'amplificateur, le câble B2 est branché via un T avec le câble C2 qui comme le câble C1 peut être branché à un oscilloscope, soit à l'acquisition soit aux deux. Le câble C3, branché sur la sortie OUTPUT du lock-in, porte le résultat du traitement du lock-in, il est branché à un oscilloscope pour voir en temps réel le niveau du courant de ions et est branché à l'acquisition de donnée.

D.3 Source

Sur l'alimentation de la source (photo D.4), sont branchés, le câble B2 qui est une sortit TTL de la polarisation de la source, le câble D1 qui polarise la grille interne de la source et les câble D2 et D3 qui porte le courant d'alimentation de l'émetteur ainsi que la polarisation de ce dernier.

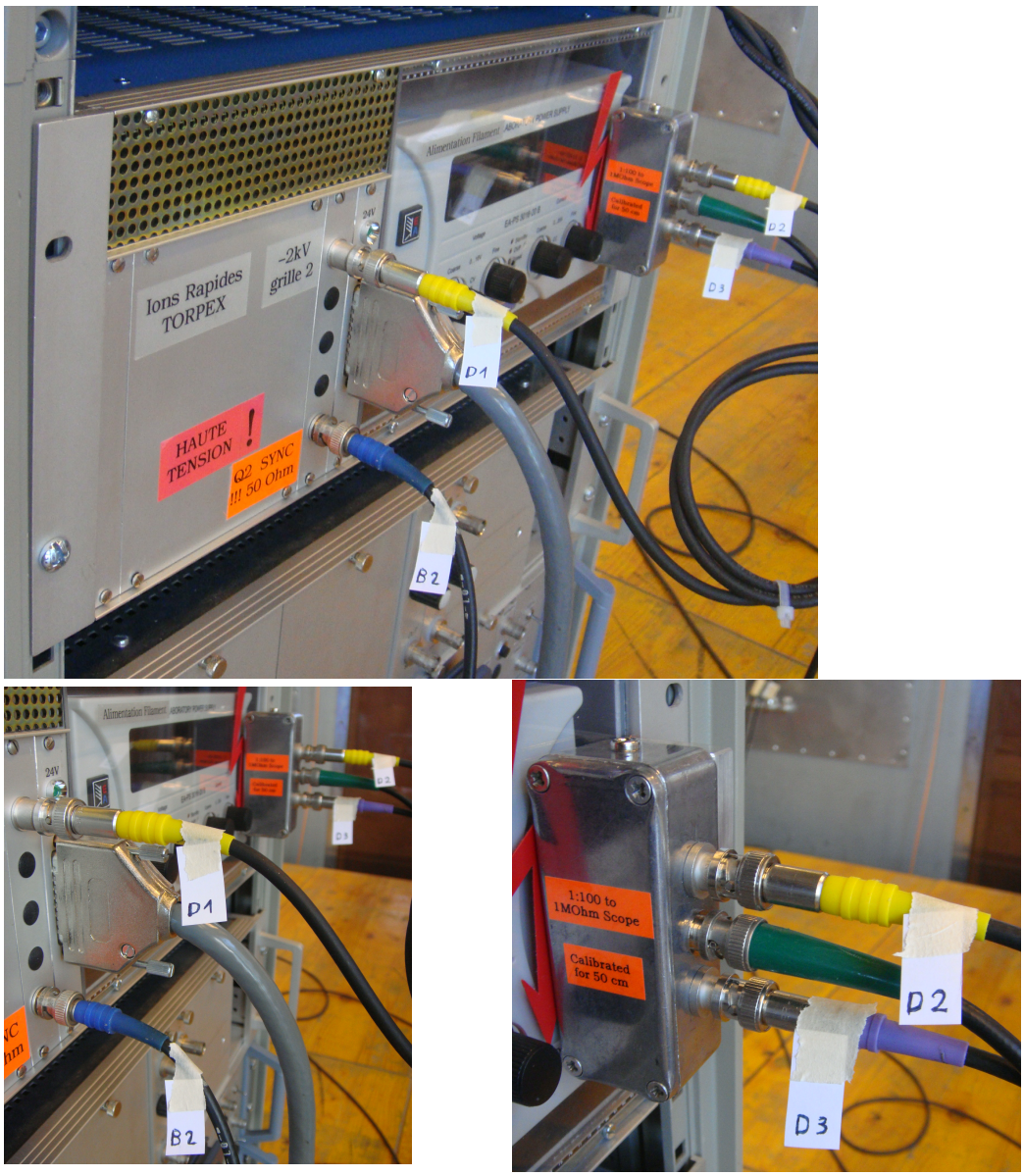

Figure D.4: Câblage de l'alimentation de la source avec zoom des différent branchements.

Bibliography

[1] "Interaction of Supra-Thermal Ions with Turbulence in a Magnetized Toroidal Plasma", Gennady Plyushchev, CRPP, EPFL, December 2009.

[2] "Operation of a 0.2-1.1 keV ion source within a magnetized laboratory plasma", H. Boehmer, D. Edrich, W. W. Heidbrink, R. McWilliams, L. Zhao and D. Leneman, University of California, 2003.

[3] "Measurements of classical transport of fast ions", L. Zhao, W. W. Heidbrink, H. Boehmer, R. McWilliams, D. Leneman and S. Vincena, University of California, 2005.

[4] "Lithium Ion Sources for Investigations of Fast Ion Transport in Magnetized Plasma", Y. Zhang, H. Boehmer, W. W. Heidbrink, R. McWilliams, D. Leneman and S. Vincena, University of California, 2007.

[5] "Experimental observation of blob generation mechanism from drift-interchange waves in a plasma", I. Furno, B. Labit, M. Podestà, A. Fasoli, S.H. Müller, F.M. Poli, P. Ricci, C. Theiler, S. Brunner, A. Diallo and J. Graves, CRPP, EPFL, June 2010.

[6] http://www.cathode.com/pdf/tb-118.pdf, Heat wave lab website.

[7] "Waves and instabilities in inhomogeneous plasmas", http://crppwww.epfl.ch/ brunner/inhomoplasma.pdf.

[8] "Simulation of the dynamics and transport of fast ions in the TORPEX turbulent plasma", Alice Burckel, CRPP, EPFL, Lausanne, January 2009.

[9] "Plasma physics via computer simulation", C. K. Bidsall and A. B. Langdon, McGraw-Hill book compagny, 1985.

[10] "U S M, ultrasonic motor General Catalogue", Shinsei Corporation, http://www.shinsei-motor.com/downloads/Catalog_E_2005_09.pdf.

Acknowledgments

I would like to thank every person who helped me during this Master project. Especially the members of the TORPEX team, lead by Prof. Ambrogio Fasoli. I am very grateful to Dr. Ivo Furno, member of this team, who particularly supported me during this semester.

I would like to thank all the crpp staff who helped me for this project, in particular; Philippe Marmillod for the development of the Lock-in device and Pierre Lavanchy for the work on the connection of the detector, from the electronics workshop; Omar Bartolomeoli for his help during the maintenance of the setup on TORPEX, from the vacuum workshop; Patrice Gorgerat for the plan of the source's toroidal moving system; and everyone I've forgotten.

Finally, I would like to thank people who supported me out of the purely physical or technical part of this work, especially Michael Boksanyi for correcting my English.